The FASEB Journal article fj.13-229948. Published online May 30, 2013.

TRPA1 controls inflammation and pruritogen responses in allergic contact dermatitis

Boyi Liu,* Jasmine Escalera,*,[1] Shrilatha Balakrishna,* Lu Fan,* Ana I. Caceres,* Eve Robinson,† Aiwei Sui,* M. Craig McKay,‡ M. Allen McAlexander,§ Christina A. Herrick,† and Sven E. Jordt*,[2]

*Department of Pharmacology and †Department of Dermatology, Yale School of Medicine, New Haven, Connecticut, USA; ‡Biological Reagents and Assay Development, GlaxoSmithKline Pharmaceuticals, Research Triangle Park, North Carolina, USA; and §Respiratory Therapy Area, GlaxoSmithKline Pharmaceuticals, King of Prussia, Pennsylvania, USA

ABSTRACT **Allergic contact dermatitis is a common skin disease associated with inflammation and persistent pruritus. Transient receptor potential (TRP) ion channels in skin-innervating sensory neurons mediate acute inflammatory and pruritic responses following exogenous stimulation and may contribute to allergic responses. Genetic ablation or pharmacological inhibition of TRPA1, but not TRPV1, inhibited skin edema, keratinocyte hyperplasia, nerve growth, leukocyte infiltration, and antihistamine-resistant scratching behavior in mice exposed to the haptens, oxazolone and urushiol, the contact allergen of poison ivy. Hapten-challenged skin of TRPA1-deficient mice contained diminished levels of inflammatory cytokines, nerve growth factor, and endogenous pruritogens, such as substance P (SP) and serotonin. TRPA1-deficient sensory neurons were defective in SP signaling, and SP-induced scratching behavior was abolished in *Trpa1*$^{-/-}$ mice. SP receptor antagonists, such as aprepitant inhibited both hapten-induced cutaneous inflammation and scratching behavior. These findings support a central role for TRPA1 and SP in the integration of immune and neuronal mechanisms leading to chronic inflammatory responses and pruritus associated with contact dermatitis.—Liu, B., Escalera, J., Balakrishna, S., Fan, L., Caceres, A. I., Robinson, E., Sui, A., McKay, M. C., McAlexander, M. A., Herrick, C. A., Jordt, S. E. TRPA1 controls inflammation and pruritogen responses in allergic contact dermatitis. *FASEB J.* 27, 000–000 (2013). www.fasebj.org**

Key Words: pruritis · sensory neurons · TRP channels

Allergic contact dermatitis (ACD) is a common skin condition characterized by contact hypersensitivity to allergens, inflammation, and pruritus. In the majority of patients, contact dermatitis is caused by sensitization and subsequent epicutaneous challenge with environmental, occupational, or nutritional allergens (1). One of the most commonly encountered contact allergens is urushiol, produced by poison ivy, oak, and sumac, affecting >10 million patients a year in the United States alone (2). Other contact allergens include metals, such as nickel and cobalt, fragrance constituents, detergents, and food chemicals. These reactive chemicals haptenate skin proteins and produce a predominantly Th_2-type allergic response. Inflammation results in the breakdown of the skin barrier and eczema. Increased contact hypersensitivity is also a hallmark of atopic dermatitis, in which mutations in the filaggrin gene lead to defects of the skin barrier (3).

One of the major characteristics of ACD is persistent pruritus, leading to scratching behavior that further damages the skin and facilitates access by allergens and pathogens (4). While the immune response in ACD has been extensively investigated, little is known about the mechanisms leading to pruritus. The sensation of itch is initiated by excitation of sensory nerve fibers innervating the inflamed skin site. These fibers are activated by inflammatory mediators released by immune cells or skin tissue cells. In chronic contact dermatitis, antihistamine treatment is oftentimes insufficient to inhibit pruritus and inflammation, leaving limited treatment options (4). The nature of the histamine-independent

Abbreviations: 5-HT, serotonin; ACD, allergic contact dermatitis; CGRP, calcitonin gene-related peptide; ddPCR, digital droplet polymerase chain reaction; DRG, dorsal root ganglion; ET-1, endothelin-1; 4-HNE, 4-hydroxynonenal; FACS, fluorescence-activated cell sorting; H&E, hematoxylin and eosin; NGF, nerve growth factor; NK_1, neurokinin 1; NK_1R, neurokinin 1 receptor; PCR, polymerase chain reaction; qPCR, quantitative polymerase chain reaction; SP, substance P; TEWL, transepidermal water loss; TRP, transient receptor potential; TRPA1, transient receptor potential cation channel, subfamily A, member 1; TRPV1, transient receptor potential cation channel, subfamily V, member 1

[1] Current address: Brain Trauma Foundation, 7 World Trade Center, 250 Greenwich St., 34th Floor, New York, NY 10007, USA.

[2] Correspondence: Department of Pharmacology, Yale School of Medicine, 333 Cedar St., New Haven, CT 06510, USA. E-mail: sven.jordt@yale.edu

doi: 10.1096/fj.13-229948

This article includes supplemental data. Please visit *http://www.fasebj.org* to obtain this information.

inflammatory and pruritic pathways in chronic dermatitis, as well as the signaling mechanisms leading to their activation, are largely unknown. In rodent models, histamine receptors have been shown to excite sensory nerve fibers through downstream activation of transient receptor potential (TRP) cation channel, subfamily V, member 1 (TRPV1) ion channels (5). A similar dual role in pain and itch transduction may apply to TRP cation channel, subfamily A, member 1 (TRPA1), another sensory TRP ion channel activated by reactive exogenous and endogenous stimuli (6–8). TRPA1 was shown to be essential for pruritus induced in mice by injection of chloroquine, the antimalarial agent known to cause itch in humans and rodents (9). Studies in mice have also shown that TRPA1 is essential for acute itch induced by injection of BAM8-22, a proenkephalin product, by injection of oxidants and of leukotriene B4 (9–11). Although these findings demonstrate that TRPA1 may contribute to acute histamine-independent itch sensations, it is unclear whether these (or other) TRPA1-activating mediators are present in ACD skin to induce chronic pruritus.

In addition to pain and itch, sensory nerves promote acute and delayed inflammatory responses in the skin in ACD and other pathological skin conditions (12). Nerve transection, anesthesia, or selective ablation of peptidergic C-fibers strongly inhibited both acute chemically induced inflammation and delayed sensitivity responses in rodent and human skin (13–15). Chemical stimulation of sensory nerve fibers triggers the local release of neuropeptides, such as substance P (SP) or calcitonin gene-related peptide (CGRP) that mediate neurogenic inflammatory responses, resulting in dilation of cutaneous vessels, plasma extravasation, and edema. The role of individual sensory TRP ion channels in the delayed type hypersensitivity response in ACD remains to be defined. Whereas TRPV1-deficient mice showed exaggerated inflammatory responses in the mouse oxazolone model of ACD, recent studies reported that TRPV1 antagonist treatment accelerated recovery of the skin barrier, and also reduced scratching behavior in ACD mouse models (16–18). TRPA1 agonists were shown to enhance cutaneous sensitization to the model hapten, FITC, in mice but not to other haptens, such as dinitrofluorobenzene (DNFB) and oxazolone (19). Direct effects of haptens on TRPA1- and TRPA1-deficient mice have not been reported.

Because of its sensitivity to multiple inflammatory mediators and its potential role in pruritus signaling, we hypothesized that TRPA1 serves as a major integrator of neuronal and immune mechanisms in ACD. Using mouse models of ACD, we demonstrate that neuronal TRPA1 channels are required for cutaneous inflammation and edema associated with both acute and chronic contact hypersensitivity, and for the elicitation of repetitive scratching behavior. These responses are likely triggered by multiple TRPA1-activating stimuli that we detected in dermatitis skin.

MATERIALS AND METHODS

Animals

Experimental procedures were approved by the Institutional Animal Care and Use Committee of Yale University. *Trpa1*$^{-/-}$ mice were a gift from David Julius (University of California, San Francisco, CA, USA). The *Trpa1*-knockout allele was backcrossed into the C57BL/6 background (>99.5%) by marker-assisted accelerated backcrossing (Charles River Laboratories, Wilmington, MA, USA). *Trpv1*$^{-/-}$ mice were purchased from Jackson Laboratories (Bar Harbor, ME, USA). C57BL/6 mice were purchased from Charles River Laboratories. Animals were matched for age (8–12 wk) and gender.

Chemicals

Oxazolone was from VWR/Alfa Aesar (Mississauga, ON, Canada). Urushiol (15:1) was from Phytolab (Vestenbergsgreuth, Germany). HC-030031 and A-967079 were custom synthesized by Medchem101 (Conshohoken, PA, USA). L733060 and GR73632 were from Tocris Bioscience (Ellisville, MO, USA). BQ-123 and AMG-9810 were from Enzo Life Science (Plymouth Meeting, PA, USA), BQ-788 was from Peptide International (Louisville, KY, USA). PGE_2 was from Cayman Chemical (Ann Arbor, MI, USA). Methyl cellulose (Methocell MC, medium viscosity, 1200–1800 mPa·s) was from Fluka (Buchs, Switzerland). All other chemicals were from Sigma-Aldrich (St. Louis, MO, USA).

Oxazolone-induced ACD model

Oxazolone was dissolved in a mixture of acetone:olive oil (4:1). Mice were sensitized with 2% oxazolone solution applied to the shaved abdomen (150 μl). 5 d later, mice were challenged with 1% oxazolone applied to the right ear, and vehicle was applied to the left ear. Ear thickness was measured before challenge, and again after challenge, at the time indicated, using a digital spring-loaded thickness gauge (Mitutoyo Quick Mini 700-118-20; Mitutoyo Corp., Kawasaki, Japan). For therapeutic intervention, the TRPA1 antagonist HC-030031 was injected (200 mg/kg, i.p.) 1 h prior to challenge and 100 mg/kg 8 and 16 h after challenge for a total of 3 injections. Methylcellulose (0.5% in water) was used as vehicle. The neurokinin 1 receptor (NK_1R) antagonist L733060 (7.5 mg/kg, vehicle: 3% DMSO, i.p.) was applied 30 min before challenge and 4, 8, 12, and 16 h postchallenge for a total of 5 injections. Punch ear biopsies (4 mm diameter; Miltex, York, PA, USA) were excised 24 h after challenge.

Oxazolone-induced chronic contact dermatitis

Mice were sensitized by applying 2% oxazolone as above. After 7 d, mice were challenged with 0.5% oxazolone dissolved in acetone (50 μl) by painting the shaved nape of the neck 3×/wk for a total of 10 times. For induction of dermatitis on the lower back, 0.5% oxazolone was applied on the shaved lower back 4× every other day.

Urushiol-induced contact dermatitis

Mice were sensitized by applying 2% urushiol (30 μl, dissolved in a 4:1 mixture of acetone:olive oil) to the shaved abdomen. After 5 d (d 0), mice were challenged with 0.5% oxazolone dissolved in acetone (30 μl) by painting the shaved nape of the neck. On d 2 and 4, mice were challenged with urushiol in the same way as d 0, for a total of 3 challenges.

Transepidermal water loss (TEWL) is measured 24 h after the last urushiol challenge using a VapoMeter (Delfin Technologies, Kuopio, Finland).

Scratching behavior analysis

The scratching behavior of mice was recorded using video cameras positioned above the observation chamber. Mice were placed in the chamber to acclimate for 60 min. Then mice were videotaped during the first and fifth hour (in some cases after 24 h) of oxazolone challenge. A series of one or more scratching movements by the hind paw directed toward the neck was defined as a scratching bout, which ended when the mouse either licked its hind paw or placed its hind paw back on the floor. The total number of scratching bouts was counted for 1 h. Drug doses chosen for testing antipruritic effects were based on previous reports. All drugs were prepared in 0.5% methylcellulose solution and injected in 5 ml/kg volume (i.p.) 45 min before the test. To study the scratching responses on pruritogen injection, the nape skin of the mouse was shaved 3 d before testing. Pruritogen dosages were chosen according to previous reports. Compounds were injected intradermally into the nape skin in a volume of 50 μl. Scratching behavior was recorded for 30 min.

Isolation of T cells from mouse ear tissue

Mice were euthanized 24 h postchallenge, and ears were dissected and minced into fragments. Ear fragments were incubated in 2 ml of digestion buffer, containing 2.7 mg/ml collagenase type IV (Sigma-Aldrich C5138-G), 1 mg/ml DNase I (Sigma-Aldrich D5025), 0.25 mg/ml hyaluronidase type IV (Sigma Aldrich H3884) in HEPES-buffered RPMI medium with pyruvate for 120 min at 37°C. The supernatant from this step was collected, and the remaining tissue fragments were crushed through a 40-μm-pore strainer to obtain additional cells. Cells were isolated by centrifugation and resuspended in HBSS for counting. One million cells from each ear were obtained for subsequent staining and fluorescence-activated cell sorting (FACS) analysis.

FACS

Cells isolated from ear tissue were prepared and stained following standard protocols for FACS analysis using the following monoclonal antibodies: CD3-FITC, CD4-Cy, and CD8-PE (from BD Biosciences, San Jose, CA, USA). The first 100 μl of cells were placed into FACS tubes (10^6 cells/ear) and blocked with 2.4G2 (1:10 dilution prepared in staining buffer) for 30 min at room temperature. Following blocking, appropriate primary antibodies were added to each tube (1:100 dilution prepared in staining buffer) for 15 min on ice protected from light. After antibody preparation, cells were fixed using 1% paraformaldehyde and stored at 4°C protected from light until use. Cells were analyzed using a FACSCalibur; dead cells or debris were eliminated by appropriate gating on forward and side scatter. Data collected were analyzed using FlowJo (TreeStar, Ashland, OR, USA) software.

Evans Blue extravasation assay

At 23 h after challenge with oxazolone, 100 μl of a 0.5% Evans Blue dye solution was injected intravenously into anesthetized mice. At 1 h after injection, the mice were perfused, and ear biopsies were excised and dried for 24 h at 55°C. Biopsies were weighed and incubated in 1 ml formamide at room temperature for 24 h to extract Evans Blue dye. Evans Blue concentration was determined fluorometrically by excitation at 620 nm and measuring fluorescence intensity at 680 nm using a Tecan Saffire plate reader (Tecan Group Ltd., Männedorf, Switzerland).

Histological and immunofluorescent analysis

Circular 4-mm punch biopsies were excised from ears and nape and fixed in 4% formaldehyde and embedded in paraffin. Sections were cut at 4 μm, mounted onto slides, and stained with hematoxylin and eosin (H&E), according to standard procedures. Eosin-positive cells were counted from 3 sections/mouse under an ×20 objective by an experimenter blinded to grouping and then averaged. Immunofluorescent staining was performed using 4-μm paraffin sections. Primary antibodies of 4-hydroxynonenal (4-HNE), PGP9.5 (Abcam, Cambridge, MA), filaggrin, loricrin, involucrin (Santa Cruz Biotechnology, Santa Cruz, CA, USA), and corresponding secondary antibodies (Invitrogen, Carlsbad, CA, USA) were used for staining. Nuclei were stained with DAPI. Images were obtained by Zeiss Imager Z1 microscope and analyzed by AxioVision Rel. 4.7 software (Zeiss, Munich, Germany). For quantification of immunofluorescent staining, 8 images were randomly selected per mouse tissue. The percentage of the staining area in each of selected images is calculated by ImageJ software and then averaged.

Bifold skin thickness, skin biopsy weight, and morphology evaluation

The increase in bifold skin thickness, as measured by the thickness gauge mentioned above, was calculated by subtracting the values before sensitization from those obtained from specific days afterward. Six determinations were made at different dorsal skin sites per mouse. For skin biopsy weight studies, eight 4-mm-diameter punches of skin throughout the entire shaved area per mouse were taken and weighed. The severity of dermatitis was scored following criteria described previously (18). Individual scores (0, none; 1, mild; 2, moderate; 3, severe) of dryness, excoriation, erythema, and edema were summed up as the dermatitis score by an experimenter blinded to genotype and treatment. Epidermal thickness in H&E-stained sections was measured at 20 points in 150-μm stepping distance throughout the section and averaged thereafter.

Skin protein isolation and ELISA

At 24 h after oxazolone challenge, mice were euthanized, and 4-mm ear biopsies were excised and immediately frozen in liquid nitrogen. Tissue was homogenized using a Bullet Blender (NextAdvance, Averill Park, NY, USA) in 50 mM Tris-base (pH 7.4) and 150 mM NaCl with protease inhibitor and 0.2% Triton-X. Homogenization was carried out 20 min at full speed. Then samples were centrifuged at 10,000 *g* for 10 min at 4°C. The supernatant was tested by ELISA for the following analytes: IL-1β, CXCL2, endothelin 1 (ET-1), SP, and IL-4 from R&D Systems (Minneapolis, MN, USA), IgE from BD Biosciences (San Diego, CA, USA); nerve growth factor (NGF) from Millipore (Billerica, MA, USA), IL-6 from Enzo (New York, NY, USA); and serotonin (5-HT) from Beckman Coulter (Brea, CA, USA). Total protein was determined by BCA assay.

Calculation of SP and 5-HT concentrations in tissues

ELISA data (mg/ml) were converted to tissue concentration (μM), according to sample weight and volume of the homogenizing buffer used. The density of the skin samples was assumed to be 1 mg/ml, and the efficiency of homogenizing was 70%.

Cell culture and Ca^{2+} imaging

Adult mouse dorsal root ganglia (DRGs) were dissociated using 0.28 Wünsch units/ml Liberase Blendzyme 1 (Roche Diagnostics, Mannheim, Germany), as described previously (7). Ca^{2+} imaging was performed 16–26 h after DRG dissection. Medium was replaced by modified standard Ringer's bath solution (in mM: 140 NaCl, 5 KCl, 2 $CaCl_2$, 2 $MgCl_2$, 10 HEPES, and 8 glucose, pH 7.4). For Ca^{2+}-free extracellular solution, $CaCl_2$ was substituted by equal molar EGTA. Cells were loaded with Fura-2-AM (10 μM; Calbiochem, La Jolla, CA, USA) for 45 min. Ratiometric Ca^{2+} imaging was performed on an Olympus IX51 microscope (Olympus, Tokyo, Japan) with a Polychrome V monochromator (Till Photonics, Munich, Germany) and a PCO Cooke Sensicam QE CCD camera and Imaging Workbench 6 imaging software (PCO AG, Kelheim, Germany). For dose-response analysis of oxazolone-induced TRPA1 activation, TRPA1-transfected HEK293T cells were superfused with oxazolone solutions (0–1 mM) for 30 s, followed with a saturating concentration of mustard oil (70 μM). Fifteen to 20 cells were analyzed for each concentration (20).

Real-time polymerase chain reaction (PCR) and digital droplet PCR (ddPCR)

Total RNA was isolated from tissue homogenates using RNeasy Mini Kit 50 (Qiagen, Valencia, CA, USA). cDNA synthesis was performed with the high-capacity RNA-to-cDNA Kit (Applied Biosystems, Foster City, CA, USA). Real-time and digital PCR was performed with the LightCycler 480 real-time PCR system (Roche, Mannheim, Germany) and QX100 Droplet Digital PCR System 9 (Bio-Rad, Richmond, CA, USA) using TaqMan gene expression assays (Applied Biosystems). For real-time quantitative PCR (qPCR), each sample was run in triplicate and normalized to GAPDH gene expression. C_T values were determined using LightCycler 480 software and averaged. Relative quantification was determined by the $\Delta\Delta C_T$ method. For ddPCR, the copy number of each cDNA was normalized with the amount of RNA (ng) used for reverse transcription. The primers used were as follows: mGAPDH (4352932), mIL-1β (Mm01336189_m1), mIL-4 (Mm00445259_m1), mNGF (Mm00443039_m1), mCXCL-2 (Mm00436450_m1), mET-1 (Mm00438656_m1), mTAC1 (Mm01166996_m1), mTRPA1 (Mm01227437_m1), mTRPV4 (Mm00499025_m1), hGAPDH (4332694), hTRPA1 (Hs00175798_m1 and Hs00929054_m1), and hTRPV4 (Hs01099348_m1). Adult/fetal human skin and DRG total RNAs were purchased from Agilent Technologies (Santa Clara, CA, USA) and Clontech (Mountain View, CA, USA).

Statistics

Statistical comparisons were made between groups using Student's *t* test (for comparison between 2 groups) or 1-way ANOVA (for comparison among ≥3 groups) followed by Tukey *post hoc* test, with values of $P < 0.05$ considered significant. Data in bar graphs are expressed as means ± SE.

RESULTS

TRPA1 hapten responsiveness and proinflammatory role in acute oxazolone-induced dermatitis in mice

We initially examined the roles of TRPA1 and TRPV1 channels in an acute oxazolone-induced model of dermatitis in mice, a model that closely recapitulates the hallmarks of ACD in human patients (21). Mice were sensitized by application of oxazolone to the abdominal skin, followed by a single challenge of the ear skin 5 d later. Wild-type mice showed a typical delayed hypersensitivity response resulting in edema formation, more than doubling ear thickness 24 h after challenge (**Fig. 1*A*, *B***). Without prior sensitization, oxazolone caused only minimal increases in ear thickness (15±5%; n=5). The weights of circular tissue biopsies taken from the challenge site more than doubled in oxazolone-challenged and -sensitized wild-type (WT) mice (Fig. 1*A*, *B*). In contrast, edema formation in *Trpa1*$^{-/-}$ mice was strongly diminished (Fig. 1*A*, *B*). Mice deficient in TRPV1 showed normal edema formation (Fig. 1*A*, *B*). Pharmacological inhibition of TRPA1 during oxazolone challenge with the TRPA1 antagonist, HC-030031, inhibited edema formation in WT mice (Fig. 1*C*, *D*). In WT mice, histopathological analysis of ear tissue biopsies detected clear signs of edema formation and eosinophilic infiltration, with characteristic formation of pustules described for this model (ref. 22 and Fig. 1*E*, *F*). Edema, eosinophilia, and pustule formation was strongly diminished in *Trpa1*$^{-/-}$ mice and WT mice treated with HC-030031 during challenge (Fig. 1*E*–*G*). Oxazolone hypersensitivity has been shown to depend on both $CD4^+$ Th1 cells and $CD8^+$ cytotoxic T cells that orchestrate the local inflammatory response in the skin (23). FACS counting of leukocytes isolated from oxazolone-challenged ear skin showed that treatment with HC-030031 strongly reduced the numbers of both effector cell populations (Fig. 1*H*) and local levels of inflammatory cytokine IL-1β (Fig. 1*I*). Pharmacological inhibition of TRPA1 also strongly reduced plasma extravasation associated with oxazolone challenge, suggesting that sensory neuropeptide release may contribute to inflammation in ACD (Fig. 1*J*).

Oxazolone is a hapten, a small reactive molecule that covalently modifies proteins in the skin, thereby triggering allergic responses. Since TRPA1 is sensitive to reactive chemical stimuli, we used fluorescent Ca^{2+} imaging in HEK293 cells to test whether oxazolone would activate TRPA1 channels. Oxazolone-activated human TRPA1 with an EC_{50} of 35 ± 5μM, while it had no effect on vector-transfected HEK293 cells up to 300 μM (Fig. 1*K*). Taken together, these results suggest that TRPA1 is a crucial component of the inflammatory response in contact dermatitis following the first cutaneous hapten challenge.

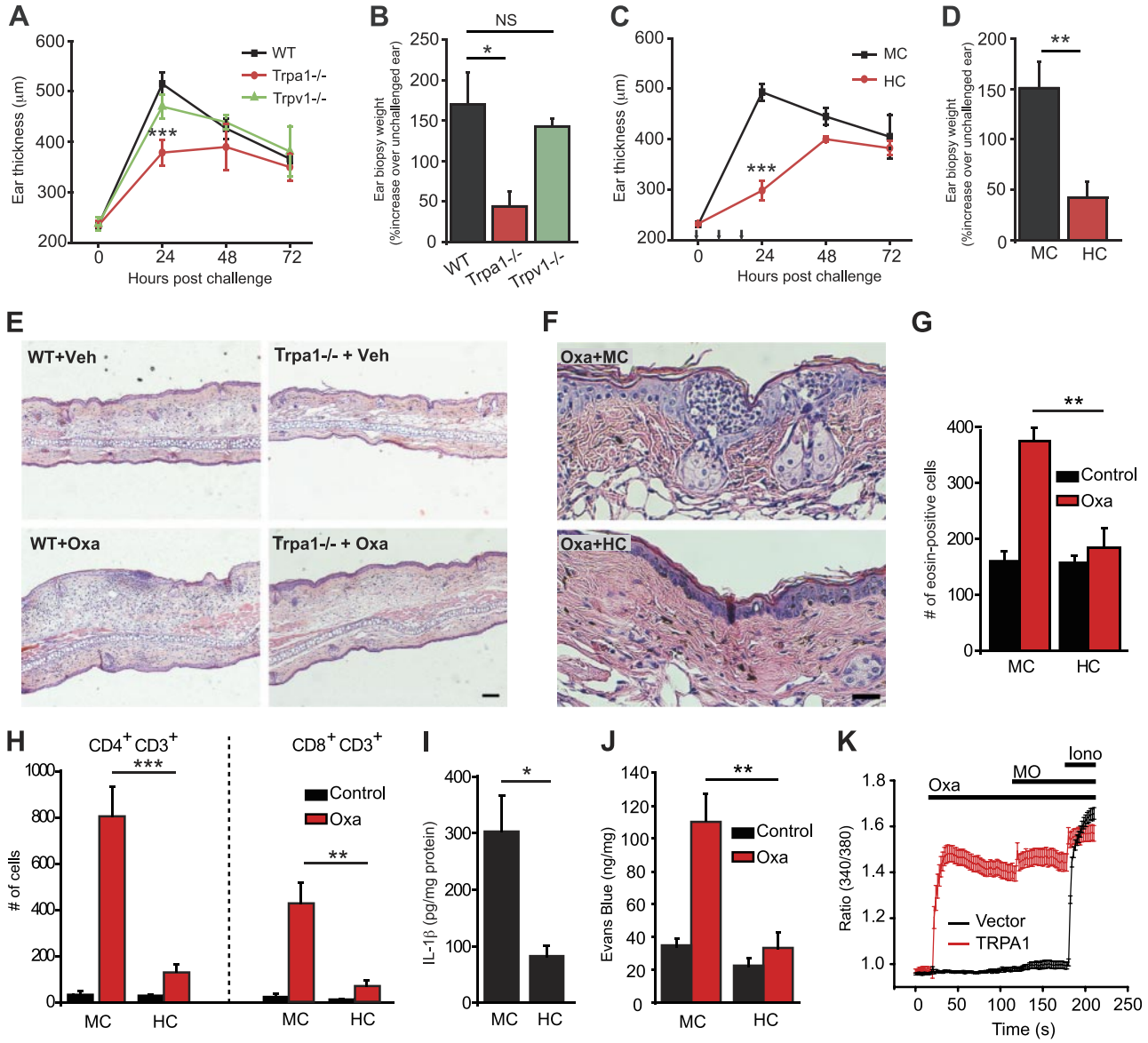

Figure 1. Diminished skin inflammation in *Trpa1*$^{-/-}$ mice, and in mice treated with TRPA1 antagonist, HC-030031, in acute oxazolone-induced dermatitis model. *A*) Ear thickness changes following challenging ear skin with 1% oxazolone, 5 d after sensitization, from C57BL/6 WT mice (black), *Trpv1*$^{-/-}$ mice (green) and *Trpa1*$^{-/-}$ mice (red). $n = 6$ mice/group. *B*) Weight differences of ear punch biopsies of oxazolone-challenged *vs.* unchallenged ears excised 24 h postchallenge from WT, *Trpa1*$^{-/-}$, and *Trpv1*$^{-/-}$ mice. $n = 6$ mice/group. *C*) Ear thickness plotted as in *A*. Measurements are shown from WT mice injected with the TRPA1 antagonist, HC-030031 (HC; red), or methyl cellulose vehicle (MC; black). $n = 6$ mice/group. Black arrows indicate time points for HC treatment. *D*) Weight differences of ear punch biopsies from oxazolone-challenged *vs.* unchallenged ears excised 24 h postchallenge from mice injected with HC or MC vehicle. $n = 11$ mice/group. *E*) H&E staining of representative mouse ear tissue sections of vehicle-treated (Veh) and oxazolone (Oxa)-challenged WT and *Trpa1*$^{-/-}$ mice. Scale bar = 100 μm. *F*) H&E staining showed diminished epidermal thickening, eosinophilia, and subepidermal pustule formation in oxazolone-sensitized and challenged mice treated with HC compared with MC. Scale bar = 25 μm. *G*) Cell counts of eosin-positive cells in sections of ear skin of mice treated with MC or HC, comparing unchallenged (control) and oxazolone-challenged ears; $n = 5$/group. *H*) $CD4^+CD3^+$ and $CD8^+CD3^+$ cells in ear tissue extracts from unchallenged and oxazolone-challenged mice treated with MC (n=8) or HC (n=9), quantified by flow cytometry. *I*) Concentrations of IL-1β in oxazolone-challenged ear tissue of MC (n=7) and HC-treated mice (n=8). *J*) Evans Blue extravasation in oxazolone-challenged and unchallenged ear tissues in mice treated with MC or HC. $n = 6$ mice/group. *K*) Oxazolone induced Ca^{2+}-responses in HEK293 cells transfected with human TRPA1 or empty vector (pcDNA3.1) measured by Fura-2 imaging. Oxazolone (Oxa; 300 μM), mustard oil (MO; 70 μM) and ionomycin (Iono; 1 μM) were applied at time points indicated by the bars. Error bars = SE (n=60 cells each). NS, not significant. *$P < 0.05$, **$P < 0.01$, ***$P < 0.001$.

Diminished chronic dermatitis pathology in *Trpa1*$^{-/-}$ mice

We next examined the role of TRPA1 in a chronic dermatitis model in which mouse neck skin is repeatedly challenged with oxazolone over weeks. In previous studies in BALB/c and hairless (*hr/hr*) mice, this model closely recapitulated important hallmarks of chronic allergic and atopic dermatitis in humans, including skin dryness, excoriation, erythema and edema, cellular inflammatory responses, and histamine-independent pruritus (21, 24). Wild-type C57BL/6 mice displayed similar outcomes in this model (**Fig. 2**). In contrast, *Trpa1*$^{-/-}$ mice showed strongly diminished dermatitis scores (Fig. 2*A*, *B*). Bifold thickness of the neck skin was reduced in *Trpa1*$^{-/-}$ mice, and skin punch biopsies from *Trpa1*$^{-/-}$ mice had lower weights than WT mice (Fig. 2*C*, *D*). H&E-stained sections of oxazolone-challenged skin showed characteristic epidermal thickening and eosinophilia in WT mice, with reduced levels in *Trpa1*$^{-/-}$ mice (Fig. 2*E*–*G*).

qPCR analysis of skin cDNA and ELISA testing of protein extracts from skin biopsies of *Trpa1*$^{-/-}$ mice revealed diminished transcriptional and protein levels of inflammatory cytokines associated with ACD (CXCL2, IL-4, and IL-6, but not IL-1β) in *Trpa1*$^{-/-}$ mice (**Fig. 3*A*, *B***). We also observed increased transcription and protein levels of NGF and SP in the skin of chronically oxazolone-challenged WT mice (Fig. 3*A*, *C*). Cutaneous levels of ET-1 and 5-HT, known to induce pain and pruritus, were also increased (Fig. 3*A*, *C*, *D*). We did not observe any increase in levels of leukotriene B4, another candidate endogenous pruritogen ($P>0.05$, $n=6$ mice/group). NGF, SP, and 5-HT levels were strongly reduced in *Trpa1*$^{-/-}$ mice in this model, but ET-1 levels were unaffected (Fig. 3*A*, *C*, *D*). Both WT and *Trpa1*$^{-/-}$ mice showed similarly elevated serum levels of IgE in the chronic oxazolone-induced dermatitis model, indicating that *Trpa1*$^{-/-}$ mice developed normal systemic immune responses to the hapten (Fig. 3*E*).

Human patients with dermatitis show increased cutaneous nerve fiber densities induced by expression of NGF (25). We therefore asked whether the reduced NGF levels in *Trpa1*$^{-/-}$ mice may lead to a decrease in

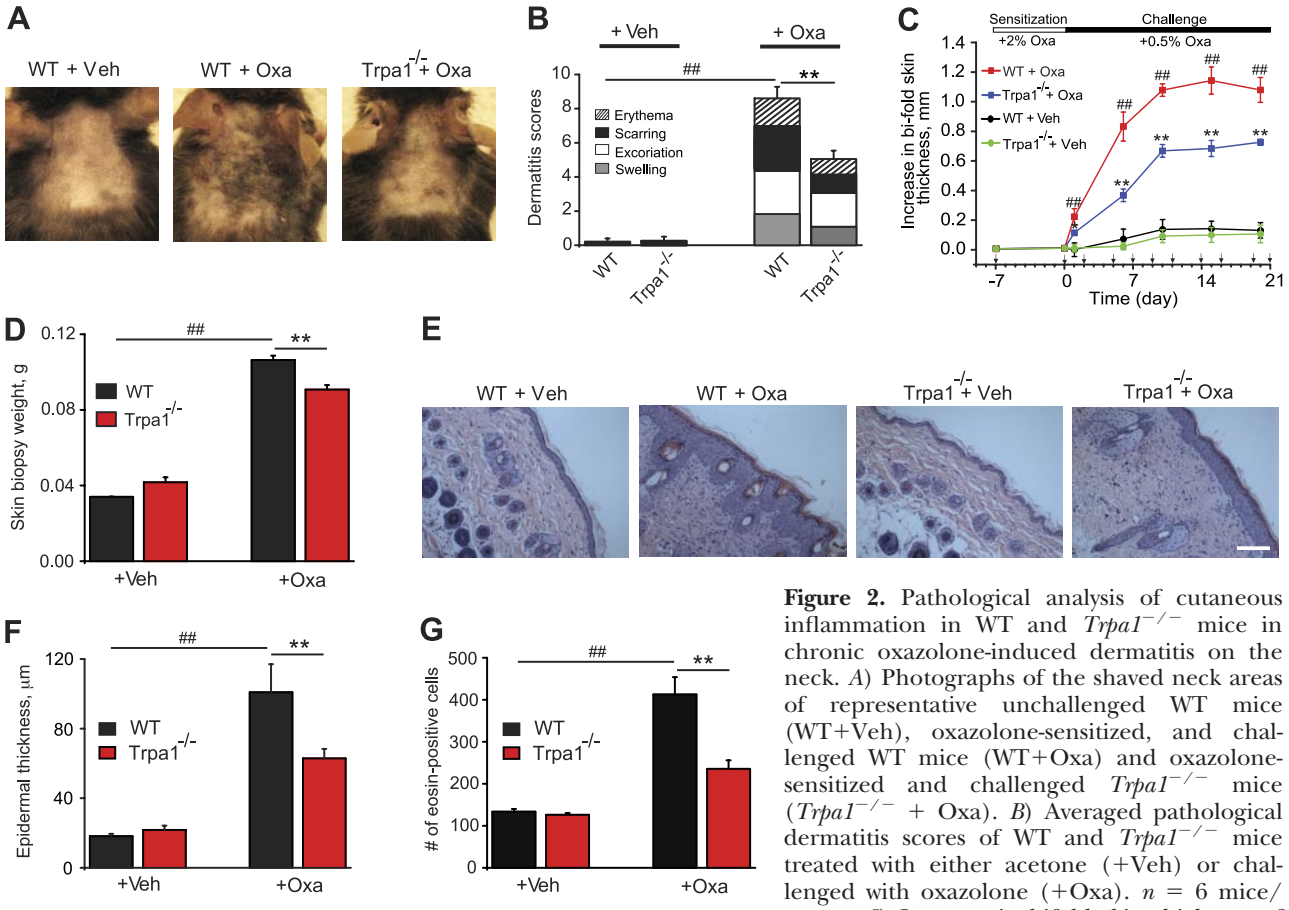

Figure 2. Pathological analysis of cutaneous inflammation in WT and *Trpa1*$^{-/-}$ mice in chronic oxazolone-induced dermatitis on the neck. *A*) Photographs of the shaved neck areas of representative unchallenged WT mice (WT+Veh), oxazolone-sensitized, and challenged WT mice (WT+Oxa) and oxazolone-sensitized and challenged *Trpa1*$^{-/-}$ mice (*Trpa1*$^{-/-}$ + Oxa). *B*) Averaged pathological dermatitis scores of WT and *Trpa1*$^{-/-}$ mice treated with either acetone (+Veh) or challenged with oxazolone (+Oxa). n = 6 mice/group. *C*) Increase in bifold skin thickness of WT and Trpa1$^{-/-}$ mice, treated with vehicle or oxazolone. Arrows indicate the days of oxazolone application. n = 6–10 mice/group. $^{**}P < 0.01$ *vs.* WT + Oxa group; $^{\#\#}P < 0.01$ *vs.* WT + Veh group. *D*) Weights of neck skin biopsies excised from WT and *Trpa1*$^{-/-}$ mice, treated with vehicle or oxazolone. n = 6–10 mice/group. *E*) H&E-stained sections of neck skin from WT and *Trpa1*$^{-/-}$ mice, treated with vehicle or with oxazolone. Scale bar = 100 μm. *F*) Measurements of epidermal thickness of WT mice and *Trpa1*$^{-/-}$ mice, treated with vehicle (acetone, left) or oxazolone (Oxa, right). n = 8–14 mice/group. *G*) Cell counts of eosin-positive cells in sections of neck skin of WT mice and *Trpa1*$^{-/-}$ mice, treated with vehicle or oxazolone, n = 6–8 mice/group. $^{**}P < 0.01$; $^{\#\#}P < 0.01$.

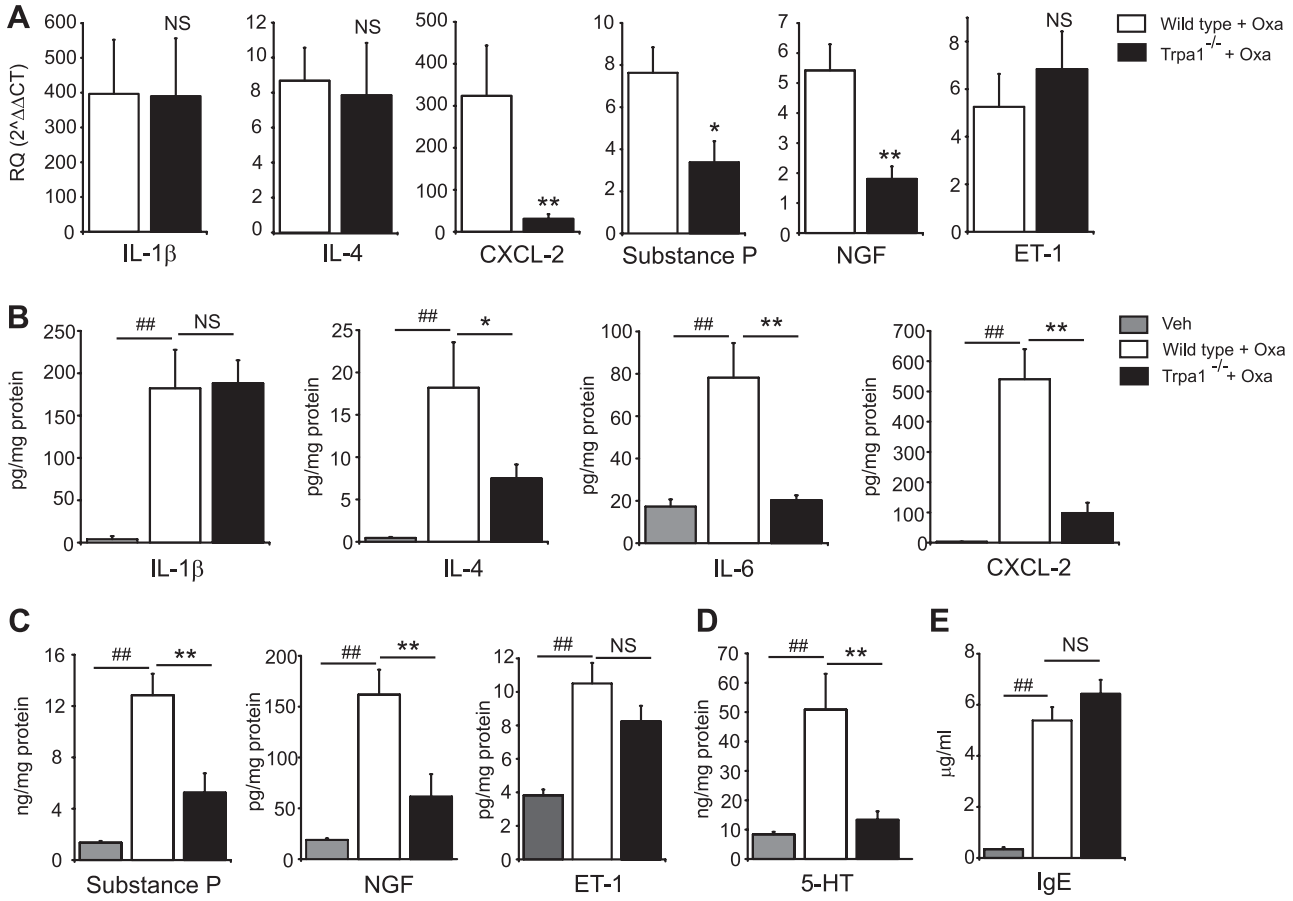

Figure 3. Expression of proinflammatory cytokines, peptide mediators, and IgE in the skin of WT and *Trpa1*$^{-/-}$ mice in the oxazolone-induced chronic dermatitis model. *A*) Relative quantities (RQ) of IL-1β, IL-4, CXCL-2, SP (tachykinin), NGF, and ET-1 gene transcripts in skin samples of oxazolone-sensitized and challenged WT (white) and *Trpa1*$^{-/-}$ mice (black), compared to levels in respective unchallenged mice (not shown), determined by TaqMan real-time qPCR. GAPDH transcript levels were used as endogenous control. $n = 8$ mice/group. *B*) Levels of cytokines IL-1β, IL-4, IL-6, CXCL-2 levels from neck skin of mice, measured by ELISA. $n = 6–10$ mice/group. *C*) Average protein concentrations of SP, NGF, ET-1 in neck skin extracts, measured by ELISA. $n = 6–10$ mice/group. *D*) Average concentration of 5-HT in neck skin extracts, measured by ELISA. $n = 6–10$ mice/group. *E*) Average serum IgE levels of unchallenged (gray) and challenged (white) WT mice, compared to levels in challenged *Trpa1*$^{-/-}$ mice (black), measured by ELISA. $n = 5–6$ mice/group. NS, not significant. $^{*}P < 0.05$, $^{**}P < 0.01$; $^{\#\#}P < 0.01$.

nerve density in mouse skin in the oxazolone dermatitis model. Indeed, immunofluorescence analysis of skin sections prepared from *Trpa1*$^{-/-}$ mice sensitized and challenged with oxazolone showed strongly diminished PGP9.5-positive nerve fibers (Supplemental Fig. S1*A*). In chronic oxazolone-induced dermatitis, epidermal hyperplasia is associated with changes in expression of structural protein markers of differentiation, including filaggrin, loricrin, and involucrin (21). The expression of these markers was strongly increased and extended into suprabasal cell layers after repetitive oxazolone challenges. In *Trpa1*$^{-/-}$ mice, expression of these markers was reduced and more restricted (Supplemental Fig. S1*B–D*).

We performed extensive qPCR and ddPCR studies to examine whether TRPA1 may be expressed locally in the skin, in addition to sensory neurons. However, all of our tests failed to detect transcription products of the TRPA1 gene in the neck skin of vehicle or oxazolone-treated mice (Supplemental Fig. S2*A*, *B*). The same probes detected TRPA1 transcripts in DRG cDNA, even when diluted in skin cDNA 5000-fold, confirming the sensitivity of the assay (Supplemental Fig. S2*C*, *D*). ddPCR analysis of mouse and human skin and DRG RNA samples also revealed much lower copy numbers of TRPA1 transcripts in skin (Supplemental Fig. S2*E*, *F*). These findings suggest that neuronal TRPA1 channels, with transcription occurring in the cell bodies of DRG neurons, were responsible for the observed cutaneous inflammatory responses.

Reduced dermatitis-associated scratching behavior in *Trpa1*$^{-/-}$ mice and in mice treated with TRPA1 antagonists

ACD is associated with the sensations of pruritus and burning originating in the affected skin regions. Similar to previous studies, we observed that mice responded with increasing numbers of scratching bouts after each oxazolone challenge of the neck skin, with

responses saturated after 10 or more challenges (Supplemental Fig. S3*A* and ref. 24). Scratching behavior was most pronounced in the first hours after challenge, followed by a gradual decline (to ~200 bouts/h), remaining at this level even 24 h later (**Fig. 4*A***). Vehicle (acetone) did not induce obvious scratching (Fig. 4*A*). *Trpa1*$^{-/-}$ mice showed ~50% decrease in scratching bouts within the first hour after challenge, and even less scratching responses at the 5th and 25th hour (Fig. 4*A*). In contrast, *Trpv1*$^{-/-}$ mice showed normal scratching behavior (Fig. 4*A*). Treatment of WT mice with the TRPA1 antagonists, HC-030031 (60 mg/kg, i.p.) or A-967079 (100 mg/kg, i.p), prior to final oxazolone challenge, similarly inhibited scratching (Fig. 4*B*, *C*). The specific TRPV1 inhibitor AMG-9810 (10 mg/kg, i.p.) had no obvious effect on scratching behavior (Fig. 4*B*, *C*). The two TRPA1 antagonists did not affect falling latencies in the rotarod test, suggesting that the observed effects on scratching were not due to alteration of motor behavior (Supplemental Fig. S3*B*). These data show that TRPA1, but not TRPV1, is also essential for the scratching behavior manifested in the oxazolone-induced chronic dermatitis model.

For analysis of pruritic responses, we also attempted to establish dermatitis by repeated application of oxazolone to a small area on the shaved mouse cheek. The cheek injection model was used in recent studies to separate acute pruritic and nocifensive behavioral responses (wiping/scratching) following injections of chemical sensory activators but has not been used for analysis of contact hypersensitivity models (10, 26). However, the allergic inflammatory response in the cheek area was highly variable and produced inconsistent repetitive behavior. For the remainder of the study, we, therefore, focused on behavior toward the neck area where consistent inflammatory and scratching responses could be induced and algesic and pruritic responses could be differentiated in previous studies (27).

It is possible that the proinflammatory effects linked to TRPA1 in the chronic oxazolone dermatitis may be caused solely by scratching-induced injury due to pruritic sensations caused by TRPA1 activity. To examine whether TRPA1 promotes cutaneous inflammation in the absence of scratching, we developed a mouse model in which oxazolone dermatitis is induced on the skin of the lower back, a site inaccessible for scratching with the hind- or forepaws of the animal (**Fig. 5*A*, *B***). In this model, oxazolone challenges induced skin thickening, erythema, swelling and excoriation, and profound transepithelial water loss and inflammation (Fig. 5*B*–*E*). All of these parameters were reduced in *Trpa1*$^{-/-}$ mice (Fig. 5*B*–*E*). These data support the idea that TRPA1 promotes inflammation in dermatitis in the absence of repetitive scratching of the affected skin site.

Increased levels of electrophilic TRPA1 agonists in dermatitis skin

In humans, dermatitis is associated with increased oxidative stress, with high levels of lipid peroxidation products enriched in the inflamed skin (28). Several of these oxidation products, including 4-HNE, have been shown to activate TRPA1 channels *in vitro* (29). We detected strongly increased levels of 4-HNE adducts in mouse skin in both acute and chronic oxazolone-induced dermatitis models. Immunofluorescence identified 4-HNE adducts in cells close to the stratum corneum, with more intense staining in suprabasal cell layers and deeper reach in the chronic dermatitis model (**Fig. 6*A*, *C***). The increase in 4-HNE adduct formation in both models was confirmed by ELISA of protein extracts from skin biopsies (Fig. 6*B*, *D*). The chronically elevated levels of oxidizing and electrophilic mediators, such as 4-HNE may increase the activity of TRPA1 channels in sensory nerves innervating the inflamed skin, resulting in burning and itching sensations associated with ACD.

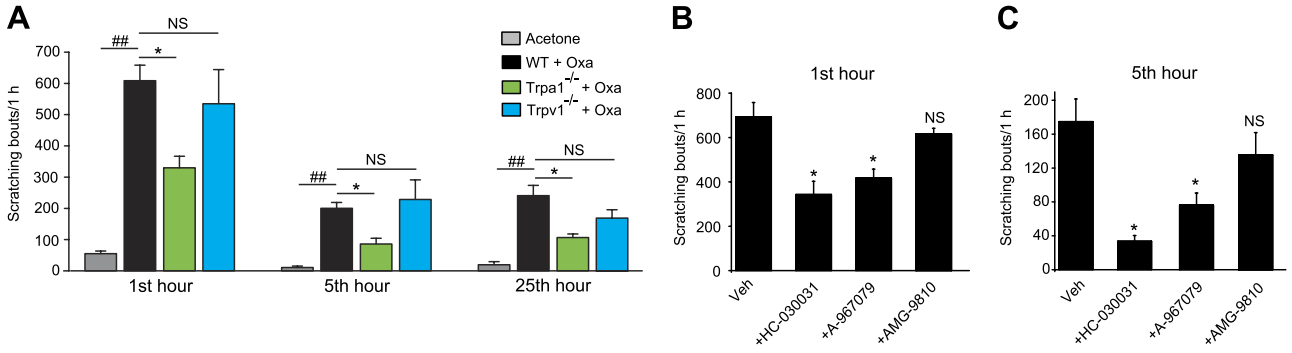

Figure 4. Contribution of sensory TRP ion channels to scratching behavior in mice in oxazolone-induced chronic dermatitis. *A*) Comparison of scratching bout numbers in WT mice treated with vehicle (acetone, gray), and oxazolone-sensitized WT (black), *Trpa1*$^{-/-}$ (green) and *Trpv1*$^{-/-}$ (blue) mice, during the 1st, 5th, and 25th hour after application of oxazolone, counted for 1 h. $n = 6$ mice/group. NS, not significant. $^{*}P < 0.05$; $^{\#\#}P < 0.01$. *B*) Numbers of scratching bouts within the first hour after application of oxazolone, counted in oxazolone-sensitized mice treated with vehicle (Veh), with TRPA1 antagonist HC-030031, TRPA1 antagonist, A-967079, or TRPV1 antagonist AMG-9810 45 min prior to challenge. $n = 6$ mice/group. *C*) Scratching bouts in the same groups of mice depicted in *B*, counted during the 5th hour following oxazolone application. Mice were injected with antagonists again 1 h before observation. $n = 6$ mice/group. $^{*}P < 0.05$ *vs.* vehicle group.

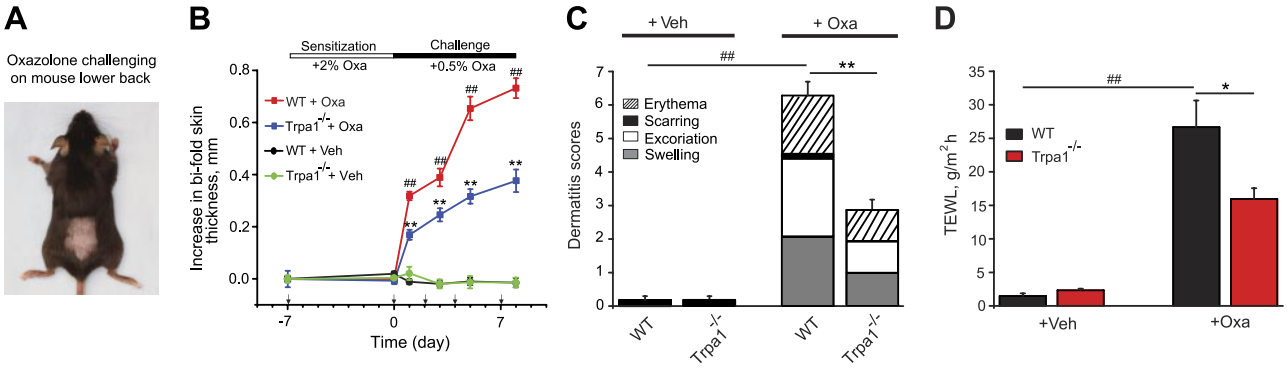

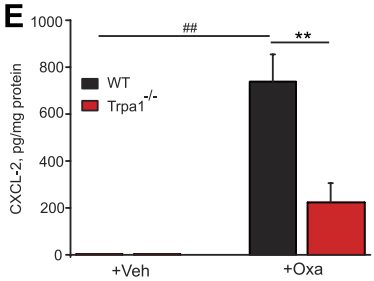

Figure 5. Analysis of dermatitis conditions in WT and *Trpa1*$^{-/-}$ mice challenged with oxazolone on the lower back. *A*) Location of the challenge site on the shaved lower back of mice. *B*) Bifold thickness of oxazolone (Oxa)- or vehicle (acetone, Veh)-challenged lower back skin in WT and *Trpa1*$^{-/-}$ mice. Arrows indicate the days of oxazolone application. $^{**}P < 0.01$ *vs.* WT + Oxa group; $^{\#\#}P < 0.01$ *vs.* WT + Veh group. *C*) Pathological dermatitis scores of WT and *Trpa1*$^{-/-}$ mice treated with either vehicle (+Veh) or challenged with oxazolone (+Oxa). *D*) TEWL of back skin of WT and *Trpa1*$^{-/-}$ mice treated with vehicle or oxazolone. *E*) Concentrations of CXCL2 in lower back skin samples of WT and *Trpa1*$^{-/-}$ mice treated with vehicle or oxazolone. $n = 6–8$ mice/group. $^{*}P < 0.05$, $^{**}P < 0.01$; $^{\#\#}P < 0.01$.

Multiple signaling pathways contribute to scratching behavior in mice in chronic dermatitis

In addition to oxidative stress, other inflammatory stimuli may increase the activity of TRPA1 to signal itch and burning sensations in dermatitis. Pruritus in chronic dermatitis is oftentimes resistant to treatment with antihistamines. Recent studies in humans and rodents identified several nonhistaminergic mediators causing acute pruritus when injected into the skin. These include SP, ET-1, 5-HT (through 5-HT$_{2A}$R) and prostaglandin E$_2$ (27, 30–32). As shown in Fig. 3, we found both SP and 5-HT to be increased in dermatitis skin, exceeding levels required for robust activation of their cognate receptors (SP: 0.8±0.1 μM, n=8 calculated from Fig. 3*C*; 5-HT: 20.4±3.3 μM, n=8, calculated from data in Fig. 3*D*, see Materials and Methods for calculation details).

Since the studies identifying the pruritic actions of these mediators used different species or mouse strains, we performed a systematic pharmacological analysis of their effects on scratching behavior in the chronic oxazolone-induced model in C57BL/6 mice. When injected prior to the last oxazolone challenge, ketanserin (3 mg/kg), a 5HT$_2$A receptor antagonist, the endothelin A (ET$_A$) receptor antagonist, BQ123 (1 mg/kg), and the NK$_1$R antagonist, L-733060 (20 mg/kg) strongly inhibited scratching behavior in this model (**Fig. 7*A*, *B***), whereas the 5HT$_3$ receptor antagonist, ondansetron (3 mg/kg), the ET$_B$ receptor antagonist, BQ788 (1 mg/kg), the NK$_2$R antagonist GR159897 (20 mg/kg) and the nonselective cyclooxygenase inhibitor indomethacin (20 mg/kg) had no effects (Fig. 7*A*, *B*). The H$_1$ histamine receptor antagonists, fexofenadine (Fexo; 10 mg/kg) and cetirizine (10 mg/kg) did not inhibit scratching behavior either, suggesting that nonhistaminergic (H$_1$) signaling dominates the behavioral responses in this model (Fig. 7*A*, *B*). The most efficacious inhibitors of scratching behavior, BQ123, ketanserin, and L733060, at the concentrations used above, did not affect motor coordination behavior in the rotarod assay (Supplemental Fig. S3*C*).

To verify whether activation of the identified pathways can induce acute scratching behavior in C57BL/6 mice, we examined responses following injections of specific activators (50 μl/site) into the nape of the neck, using dosages reported to induce scratching. Mice responded with scratching behavior to 5-HT (100 nmol), α-Me-5HT (100 nmol), SP (75 nmol), and histamine (50 μg, control) (Fig. 7*C*). Injection of other candidate pruritogens, bethanechol (Beth; 100 nmol), vasoactive intestinal peptide (VIP; 10 nmol), prostaglandin E$_2$ (PGE$_2$; 50 nmol) or the thromboxane A2 analog, U-46619 (10 nmol) failed to produce scratching behavior (Fig. 7*C* and refs. 33–35). We omitted ET-1 in these tests since it was recently found to signal through pathways not involving TRPA1 (36).

Diminished SP-induced scratching behavior and neuronal excitation in *Trpa1*-deficient mice

Next, we examined whether TRPA1 is required for the induction of scratching by 5-HT or SP that both signal through G-protein-coupled receptor pathways. Injection of α-Me-5HT (100 nmol) caused robust scratching behavior in both WT and *Trpa1*$^{-/-}$ mice (Fig. 7*D*). In contrast, SP-induced scratching behavior (75 nmol) was strongly reduced in *Trpa1*$^{-/-}$ mice (Fig. 7*E*). These findings suggest that TRPA1 may act downstream of cutaneous SP to induce scratching behavior. Skin-innervating sensory nerves are known to express NK$_1$Rs (37, 38). Activation of these receptors in cultured DRG neurons was reported to cause neuronal excitation, Ca^{2+} influx through nonselective cation channels, and neuropeptide release (39–41). Population analysis of

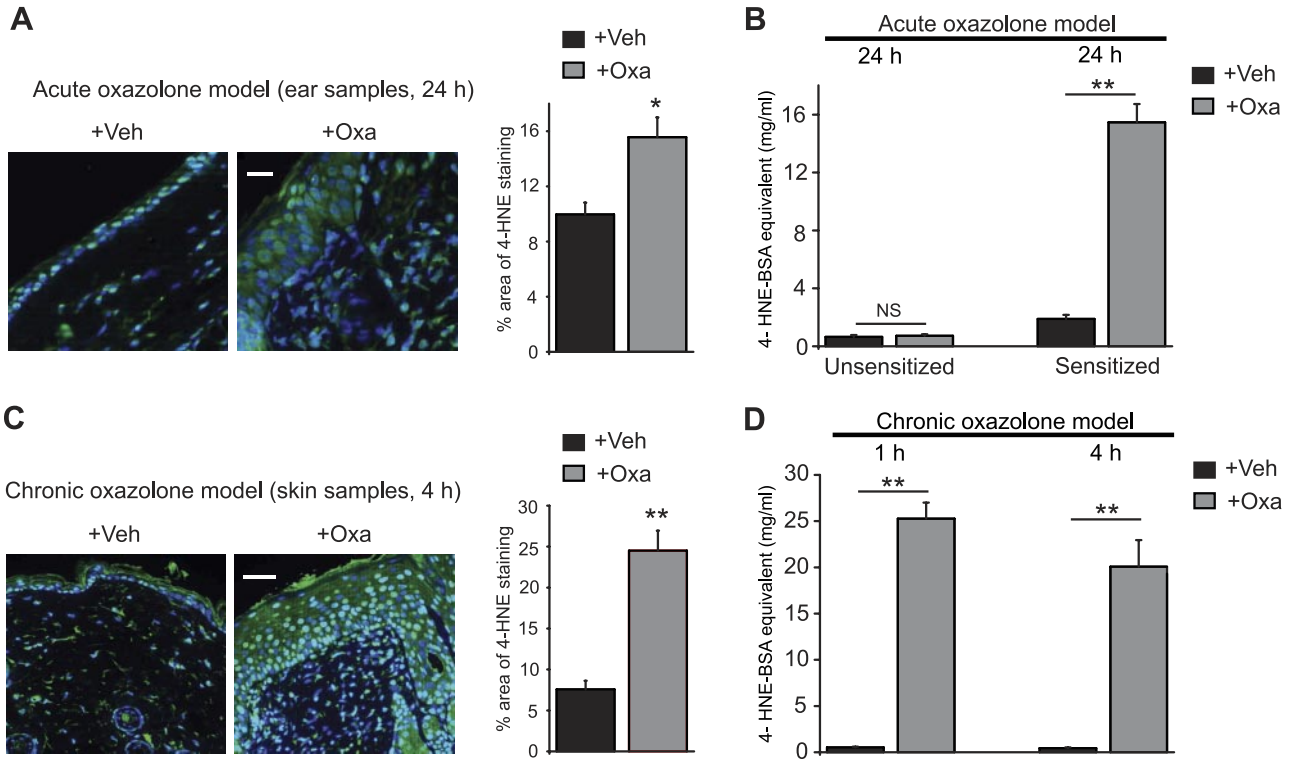

Figure 6. Skin tissue levels of 4-HNE, an endogenous TRPA1 agonist, in mouse models of acute and chronic oxazolone-induced dermatitis. *A*) Representative immunofluorescence images of 4-HNE adducts in ear skin sections of mice acutely challenged with acetone (Veh) or 1% oxazolone (Oxa). Ear biopsies were collected 24 h after challenge. Areas staining positive for 4-HNE histidine adduct are shown in green. Nuclei were labeled with DAPI (blue). $n = 5$ mice/group. *B*) 4-HNE adducts levels ear biopsies from mice in acute oxazolone-induced dermatitis model, determined by ELISA. The mice labeled as unsensitized did not receive oxazolone sensitization but were challenged with a single 1% oxazolone or vehicle on the ear. $n = 6–10$ mice/group. *C*) Representative immunofluorescence images of 4-HNE adducts in neck skin sections of oxazolone-sensitized mice chronically challenged with acetone (Veh) or 0.5% oxazolone (Oxa) on the neck skin. Skin biopsies were collected 4 h after the final (10th) challenge to the skin. $n = 6$ mice/group. *D*) 4-HNE adducts levels of neck skin from mice in chronic oxazolone-induced dermatitis model, determined by ELISA. Biopsies were collected 1 or 4 h after the final challenge (10th). $n = 8–10$ mice/group. NS, not significant. $*P < 0.05$, $**P < 0.01$.

cultured DRG neurons by fluorescent Ca^{2+} imaging showed that SP initiated Ca^{2+}-influx in 17.4 ± 2.0% of neurons (Fig. 7*F*). SP-responsive neurons were divided into 2 major categories, a larger population responsive to capsaicin and mustard oil, and a relatively smaller population unresponsive to these C-fiber activators (Fig. 7*F*). The number of SP-responsive cells was strongly diminished by the NK_1R antagonist, L733060, and the responsiveness depended on the presence of extracellular Ca^{2+} (Fig. 7*G*). The nonspecific Ca^{2+} (and TRP) channel blocker ruthenium red inhibited Ca^{2+} influx. The TRPA1 antagonist HC-030031 also diminished the numbers of SP-responsive cells. In TRPA1-deficient mice, numbers of SP-responsive neurons were similarly reduced (Fig. 7*G*). In the remaining SP-sensitive neurons in *Trpa1*$^{-/-}$ mice, SP-elicited Ca^{2+} responses were diminished (ratio increase by 0.67±0.04 in wild type, n=106 neurons *vs.* 0.53±0.03 in *Trpa1*$^{-/-}$, n=88 neurons, P<0.05). In control experiments, *Trpa1*$^{-/-}$ neurons showed normal Ca^{2+}-responses to capsaicin (ratio increase by 1.33±0.03, n=245 neurons in wild type *vs.* 1.32±0.04 in *Trpa1*$^{-/-}$, n=233 neurons, P>0.05).

NK_1R antagonists reduce dermatitis-related skin inflammation and pruritus

Since NK_1R inhibition most effectively suppressed dermatitis-associated scratching behavior, we also examined the effects of L733060 and aprepitant, a FDA-approved NK_1R antagonist that showed antipruritic and anti-inflammatory effects in human case studies on skin inflammation and pruritus. L73360 reduced edema formation and inflammatory chemokine production in acute oxazolone-challenged mouse ear tissue (Supplemental Fig. S4*A–C*). Aprepitant, administered daily during the second half of the chronic oxazolone challenge phase, also significantly reduced pathological dermatitis scores and skin thickening, and inhibited scratching behavior (Supplemental Fig. S4*D–H*).

TRPA1-dependent edema, scratching, and inflammation in dermatitis caused by urushiol, the poison ivy allergen

To examine the role of TRPA1 in contact dermatitis elicited by a clinically relevant allergen, we compared

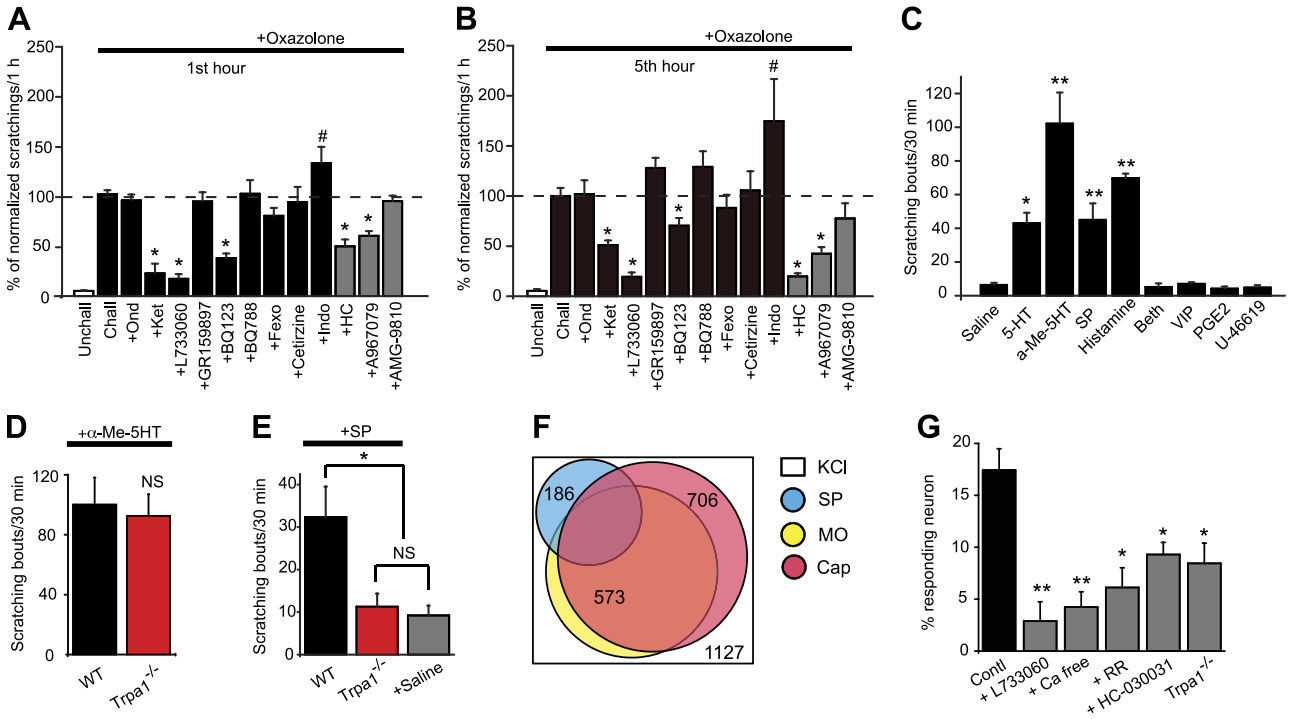

Figure 7. Pharmacological analysis of pruritogenic signaling pathways in dermatitis-induced and acute scratching behavior. *A*) Comparison of antipruritic actions of $5HT_3$ receptor antagonist ondansetron (Ond), $5HT_{2A}$ receptor antagonist ketanserin (Ket), ET_A and ET_B receptor antagonists BQ123 and BQ788, NK_1R and NK_2R antagonists L733060 and GR159897, H_1 receptor antagonists fexofenadine (Fexo) and cetirizine, nonselective cyclooxygenase inhibitor indomethacin (Indo), and TRPA1 and TRPV1 antagonists (gray) during the first hour after oxazolone challenge of the neck skin. Treatments were injected 45 min before oxazolone challenge. Counts of scratching bouts of mice treated with different antagonists were normalized to those of the corresponding vehicle-treated oxazolone-challenged mice (Chall). Unchallanged (Unchall) represents behavior of mice treated with acetone alone. (n=6–12 mice/group). Dotted line represents the 100% value. $^*P < 0.05$, $^{\#}P < 0.05$ *vs.* Chall group. *B*) Scratching behavior in the same mice as in *A*, analyzed within the 5th hour after oxazolone challenge. *C*) Scratching behaviors of C57BL/6 mice in response to candidate pruritogens. WT mice received intradermal injection of 5-HT, α-Me-5HT, SP, histamine, bethanechol (Beth), vasoactive intestinal peptide (VIP), prostaglandin E_2 (PGE_2), or U46619 into nape of neck. n = 5–8 mice/group. $^*P < 0.05$, $^{**}P < 0.01$ *vs.* saline group. *D*) Scratching bouts in WT and *Trpa1*$^{-/-}$ mice within 30 min following subcutaneous injection of α-Me-5HT into the nape of the neck. NS, not significant; n = 6 mice each. *E*) As in *D*, subcutaneous injection of SP or saline into the nape of the neck. n = 9, 16, and 14 for saline, WT and *Trpa1*$^{-/-}$ groups. *F*) Venn diagram showing quantities and overlap of neuronal populations responding to SP, mustard oil (MO) and capsaicin (Cap) in cultured DRG neurons dissociated from C57BL/6 mice. Size and overlaps of populations are indicated by circles drawn according to scale (neurons were pooled from 3 mice). *G*) Percentages of DRG neurons responding to SP (10 μM) from WT mice in vehicle (Contl), L733060 (10 μM), Ca^{2+}-free extracellular solution, ruthenium red (RR, 15 μM), HC-030031 (100 μM) treated condition, and from *Trpa1*$^{-/-}$ mice. Neurons were identified through responsiveness by final application of 30 mM KCl; 6–18 fields of observation were included in each group (each group containing 300 to 1000 neurons from 2 to 3 mice). A neuron was considered SP responsive if the peak Ca^{2+} response was >20% of the baseline. $^*P < 0.05$, $^{**}P < 0.01$ *vs.* Contl group.

the responses of WT and *Trpa1*$^{-/-}$ mice to urushiol, the allergen of poison ivy, oak, and sumac (42). Sensitization and challenge of the mouse neck skin with urushiol produced a strong increase in skin bifold thickness, indicating edema formation (**Fig. 8*A***). This response was reduced in *Trpa1*$^{-/-}$ mice (Fig. 8*A*). Urushiol challenge also caused transerpidermal water loss (TEWL), indicating disruption of the skin barrier typical for contact dermatitis (Fig. 8*B*). TEWL was diminished in urushiol-challenged *Trpa1*$^{-/-}$ mice (Fig. 8*B*). Previous studies examining urushiol's effects in mice did not examine pruritic responses (42, 43). We observed significant scratching responses toward the neck area on urushiol challenge, with diminished scratching frequencies in *Trpa1*$^{-/-}$ mice (Fig. 8*C*). Pathological analysis of urushiol-challenged neck skin showed epidermal thickening and increased eosin staining, with less thickening in *Trpa1*$^{-/-}$ mice (Fig. 8*D*, *E*). Urushiol-challenged skin contained high levels of IL-1β, with diminished levels in *Trpa1*$^{-/-}$ mice (Fig. 8*F*).

DISCUSSION

One of the major obstacles for the therapy of contact dermatitis is histamine-independent inflammation and pruritus. Here, we identified the sensory neuronal ion channel, TRPA1, as a major integrator of histamine-independent inflammatory and pruritogenic signals in murine contact dermatitis models. In the acute and chronic oxazolone-induced models, Trpa1$^{-/-}$ mice

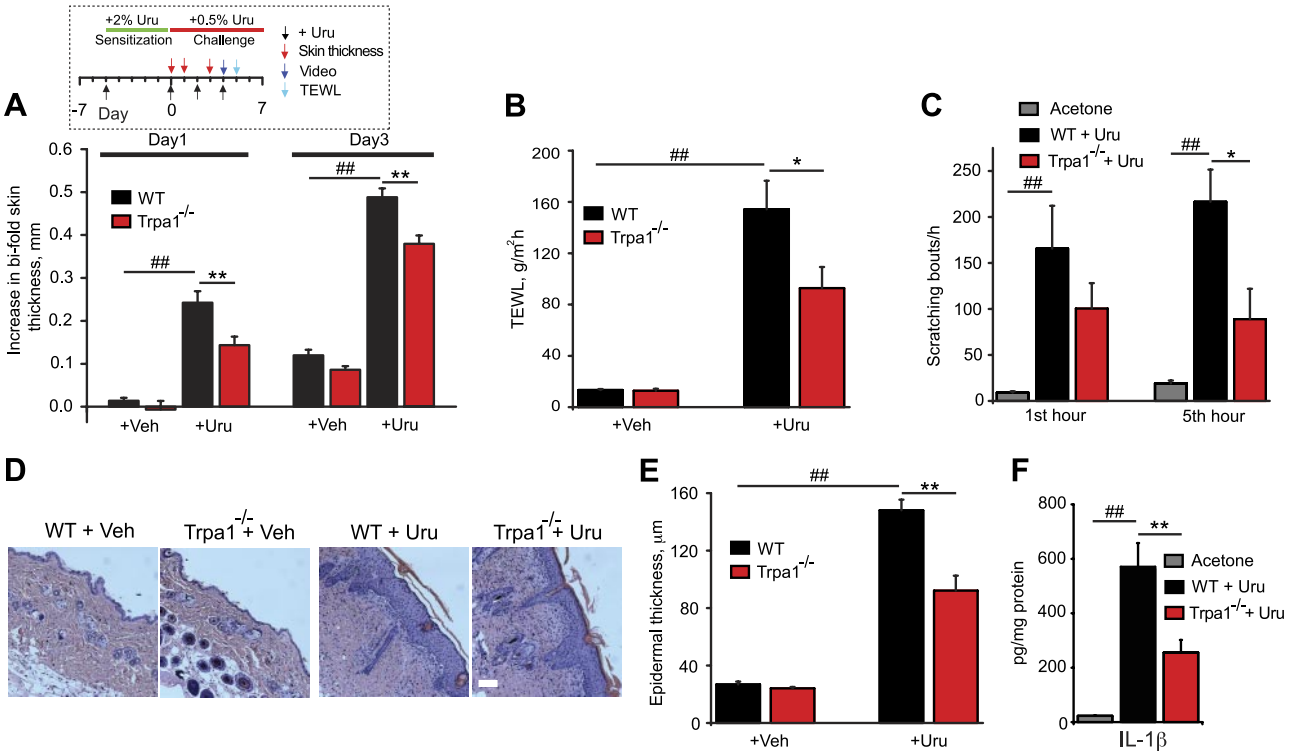

Figure 8. Analysis of cutaneous inflammation and scratching behavior in WT and *Trpa1*$^{-/-}$ mice in urushiol-induced dermatitis. *A*) Increase in bifold skin thickness of WT and *Trpa1*$^{-/-}$ mice, treated with acetone (Veh) or urushiol (Uru), on d 1 and 3. Inset: scheme of sensitization/challenge of mice with urushiol and time points for measurements. *B*) TEWL measured 24 h after the last urushiol challenge in WT and *Trpa1*$^{-/-}$ mice. *C*) Numbers of scratching bouts within the 1st and 5th hour after acetone or urushiol application to the neck. *D*) H&E stained sections of neck skin from WT and Trpa1$^{-/-}$ mice treated with acetone or urushiol. Scale bar = 100 µm. *E*) Epidermal skin thickness measured from WT and *Trpa1*$^{-/-}$ mice treated with acetone or urushiol. *F*) Concentrations of IL-1β in skin samples of WT and *Trpa1*$^{-/-}$ mice, treated with acetone or urushiol, measured by ELISA. $n = 7$ mice/group. $^{*}P < 0.05$, $^{**}P < 0.01$; $^{\#\#}P < 0.01$.

showed a general decrease in levels of critical proinflammatory cytokines, such as IL-4, IL-6, and CXCL-2. *Trpa1*$^{-/-}$ mice displayed lower dermatitis scores and diminished edema formation and thickening of the hapten-challenged skin. Genetic deletion of TRPA1 or its pharmacological inhibition reduced eosinophilia, pustule formation, plasma extravasation, and skin infiltration by T-cells. In oxazolone-challenged *Trpa1*$^{-/-}$ mice, serum IgE concentrations remained as high as in WT mice, confirming a robust systemic immune response to hapten exposure. However, inhibition of TRPA1, or its genetic deletion, prevented this response from being translated into the typical local inflammatory response at the site of hapten challenge.

How does TRPA1 promote local inflammatory responses to haptens in a sensitized animal? The acute elicitation phase of hapten-induced contact dermatitis is characterized by an early antigen-nonspecific inflammatory response, followed by a T-cell-directed antigen-specific response (44). The T-cell-directed antigen-specific response only occurs when a sufficient quantity of hapten activate the nonspecific response or when subthreshold amounts of hapten are applied together with a chemical irritant serving as an adjuvant (45). As demonstrated in the present study, TRPA1 is directly activated by oxazolone and may, thus, be activated when the hapten is applied to the skin. Oxazolone challenge likely triggers the release of proinflammatory neuropeptides, including CGRP, SP, and neurokinin A, which depend on TRPA1 to be released *in vivo* (46). This proinflammatory effect likely occurs concomitantly to the hapten-induced production of cytokines by keratinocytes and activation of mast cells through damage signals, both critical components of the early non-antigen-specific inflammatory response (44). Sensory neuropeptides are also known to modulate the function of antigen-presenting cells crucial for the initiation of the T-cell-mediated antigen-specific response following hapten challenge that we found to be diminished on TRPA1 inhibition in the acute oxazolone-induced dermatitis model (47). Together, the innate and adaptive immune responses during elicitation of contact dermatitis begin producing a wide range of stimuli activating TRPA1, including reactive oxidative species and lipid peroxidation products, such as 4-HNE, which we found to be strongly elevated in dermatitis skin.

Our data also support the notion that constant TRPA1-dependent activation of and feedback from sensory neurons is necessary to maintain chronic dermatitis and establish chronic pruritus, with SP playing a key role in histamine (and mast cell)-independent inflammation and pruritus (48–51). While TRPA1 is known to be involved in the neurogenic release of SP,

we now show that TRPA1 is also essential for SP-induced signaling in sensory neurons. Repeated oxazolone challenges led to a dramatic increase in local cutaneous expression of SP, with concentrations exceeding the reported levels required for activation of murine NK_1Rs (52). NK_1Rs are expressed in peptidergic unmyelinated peripheral sensory nerves known to transmit algogenic and pruritic signals (37, 38). Activation of NK_1Rs in cultured DRG neurons triggers action potentials and Ca^{2+} influx through nonselective cation channels (39–41). We observed that DRGs from *Trpa1*$^{-/-}$ mice contained smaller numbers of SP-responsive neurons, and the average amplitudes of the remaining SP-induced Ca^{2+}-signals were diminished, suggesting that TRPA1 contributes to SP-induced signaling. Pharmacological inhibition of TRPA1 also strongly reduced SP-elicited neuronal responses. Antagonists of NK_1Rs were initially developed as analgesics or anti-inflammatory treatments for conditions such as asthma. However, clinical trials had disappointing outcomes. The only NK_1R antagonist in current clinical use is aprepitant, approved for the prevention of chemotherapy-induced nausea and vomiting (53). Interestingly, a recent case study reported that aprepitant treatment diminished pruritus in patients suffering from Sézary syndrome, a cutaneous T-cell lymphoma associated with severe pruritus (54). Aprepitant also prevented pruritus and skin rash associated with atopic disease and with erlotinib treatment for lung cancer (55–57). While the patient numbers in these studies were small, these observations have revived interest in the blockade of NK_1Rs as an antipruritic and anti-inflammatory treatment strategy (58). Data from our present study suggest that inhibition of NK_1Rs may also counteract pruritus and inflammation in ACD. TRPA1 is likely not the only mediator of SP-induced inflammation and pruritus since L-733060, a highly efficacious inhibitor of rodent NK_1Rs, had stronger effects on cutaneous inflammation and scratching behavior than TRPA1 inhibition. SP may affect neuronal function indirectly by triggering the release of excitatory mediators from skin-resident cells (33, 48).

We also began examining the role of TRPA1 in contact dermatitis elicited by urushiol, the contact allergen of poison ivy, oak, and sumac. Dermal exposure to urushiol is the most frequent cause of contact dermatitis in the United States. In sensitized individuals, urushiol induces severe cutaneous inflammation, blistering, and pruritus, with symptoms lasting for weeks. Current therapeutic regimens are only supportive and are not directed against mechanistic targets, focusing on the removal of allergen, steroid treatment against inflammation, local anesthetics, and over-the-counter remedies against pruritus with little proven efficacy. TRPA1-deficient mice showed diminished edema formation, inflammation, skin barrier damage, and scratching behavior when challenged with urushiol, suggesting that inhibition of TRPA1 may be a novel strategy to interfere with the disease process of poison ivy-induced contact dermatitis.

Recent reports detected TRPA1 immunoreactivity in human skin, suggesting that TRPA1 may function as an irritant receptor in skin cells (59). However, tests of antibody specificity and comparisons to neuronal tissues, such as DRGs, were not presented, and other studies detected major TRPA1 expression neither in skin nor in cells of the immune system, including eosinophils, T cells, or mast cells (46, 60, 61). Our real-time qPCR and digital PCR tests, using independent hydrolysis probes and DRG control dilutions, did not detect significant local transcription of TRPA1 in skin samples from mice and humans, while cDNAs of other TRP channels, such as TRPV4, were readily detected. Further analysis of TRPA1 expression is needed, and it remains possible that both neuronal and skin-derived TRPA1 contribute to the observed phenotypes.

In addition to SP, we detected other endogenous pruritogens in chronically oxazolone-challenged dermatitis skin, including the transmitters, 5-HT, and ET-1. Previous studies have shown that subcutaneous injections of these agents cause acute pruritus in humans and scratching behavior in mice (31, 62–65). In our study, cutaneous 5-HT levels exceeded concentrations required for activation of $5\text{-}HT_{2A}$ receptors. Inhibition of $5\text{-}HT_{2A}$ receptors with ketanserin, or ET-1 receptors with BQ123 strongly inhibited hapten challenge-induced scratching behavior, almost as effectively as treatment with the NK_1R antagonist, L-733060. Cutaneous 5-HT levels were strongly reduced in oxazolone challenged *Trpa1*$^{-/-}$ mice, suggesting that sensory neuronal mechanisms control the production of 5-HT in the skin. 5-HT is produced by several skin-resident cell types, including keratinocytes, melanocytes, and immune cells, that may be affected in their functions by TRPA1 activation (66). 5-HT is also present in platelets that were found to accumulate in the skin of patients with dermatitis (67).

Neuronal and immunological responses to reactive haptens may fulfill protective functions, with scratching behavior helping to remove toxic haptens from the affected skin (68). However, chronically exaggerated allergic conditions, such as ACD, have severely negative effects on quality of life and represent a huge burden on health care systems. In many cases, causative allergens remain unknown or cannot be avoided, causing chronic inflammation and histamine-resistant pruritus. We have shown that TRPA1 is crucial to establish exaggerated neuronal and inflammatory responses against haptens and protein antigens. The inhibition of TRPA1 and TRPA1-activating signaling systems, such as the SP/NK_1R system, may represent a new therapeutic approach to disrupt the crosstalk between the nervous and immune systems to reduce inflammation and pruritus. FJ

The authors are grateful to David Julius (University of California, San Francisco, CA, USA) for *Trpa1*$^{-/-}$ mice, and to Jaime Garcia-Anoveros (Northwestern University, Chicago, IL, USA) for mouse TRPA1 cDNA. This work was funded by grants from the U.S. National Institute of Environmental

Health Sciences (awards R01 ES015056 and U01 ES015674 to S.E.J. and predoctoral fellowship F31 ES015932 to J. E.). S.E.J. is serving on the scientific advisory board of, and has equity interest in, Hydra Biosciences (Cambridge, MA, USA), a biotechnology company developing TRP channel inhibitors. Authors affiliated with GlaxoSmithKline may have equity interest in GlaxoSmithKline.

REFERENCES

1. Leung, D. Y. (2000) Atopic dermatitis: new insights and opportunities for therapeutic intervention. *J. Allergy Clin. Immunol.* **105,** 860–876
2. Gladman, A. C. (2006) Toxicodendron dermatitis: poison ivy, oak, and sumac. *Wilderness Environ. Med.* **17,** 120–128
3. Irvine, A. D., McLean, W. H., and Leung, D. Y. (2011) Filaggrin mutations associated with skin and allergic diseases. *N. Engl. J. Med.* **365,** 1315–1327
4. Buddenkotte, J., and Steinhoff, M. (2010) Pathophysiology and therapy of pruritus in allergic and atopic diseases. *Allergy* **65,** 805–821
5. Shim, W. S., Tak, M. H., Lee, M. H., Kim, M., Koo, J. Y., Lee, C. H., and Oh, U. (2007) TRPV1 mediates histamine-induced itching via the activation of phospholipase A2 and 12-lipoxygenase. *J. Neurosci.* **27,** 2331–2337
6. Jordt, S. E., Bautista, D. M., Chuang, H. H., McKemy, D. D., Zygmunt, P. M., Hogestatt, E. D., Meng, I. D., and Julius, D. (2004) Mustard oils and cannabinoids excite sensory nerve fibres through the TRP channel ANKTM1. *Nature* **427,** 260–265
7. Bessac, B. F., Sivula, M., von Hehn, C. A., Caceres, A. I., Escalera, J., and Jordt, S. E. (2009) Transient receptor potential ankyrin 1 antagonists block the noxious effects of toxic industrial isocyanates and tear gases. *FASEB J.* **23,** 1102–1114
8. Bautista, D. M., Jordt, S. E., Nikai, T., Tsuruda, P. R., Read, A. J., Poblete, J., Yamoah, E. N., Basbaum, A. I., and Julius, D. (2006) TRPA1 mediates the inflammatory actions of environmental irritants and proalgesic agents. *Cell* **124,** 1269–1282
9. Wilson, S. R., Gerhold, K. A., Bifolck-Fisher, A., Liu, Q., Patel, K. N., Dong, X., and Bautista, D. M. (2011) TRPA1 is required for histamine-independent, Mas-related G protein-coupled receptor-mediated itch. *Nat. Neurosci.* **14,** 595–602
10. Liu, T., and Ji, R. R. (2012) Oxidative stress induces itch via activation of transient receptor potential subtype ankyrin 1 in mice. *Neurosci. Bull.* **28,** 145–154
11. Fernandes, E. S., Vong, C. T., Quek, S., Cheong, J., Awal, S., Gentry, C., Aubdool, A. A., Liang, L., Bodkin, J. V., Bevan, S., Heads, R., and Brain, S. D. (2012) Superoxide generation and leukocyte accumulation: key elements in the mediation of leukotriene B4-induced itch by transient receptor potential ankyrin 1 and transient receptor potential vanilloid 1. *FASEB J.* **27,** 1664–1673
12. Roosterman, D., Goerge, T., Schneider, S. W., Bunnett, N. W., and Steinhoff, M. (2006) Neuronal control of skin function: the skin as a neuroimmunoendocrine organ. *Physiol. Rev.* **86,** 1309–1379
13. Ratzlaff, R. E., Cavanaugh, V. J., Miller, G. W., and Oakes, S. G. (1992) Evidence of a neurogenic component during IgE-mediated inflammation in mouse skin. *J. Neuroimmunol.* **41,** 89–96
14. Dux, M., Jancso, G., Sann, H., and Pierau, F. K. (1996) Inhibition of the neurogenic inflammatory response by lidocaine in rat skin. *Inflamm. Res.* **45,** 10–13
15. Beresford, L., Orange, O., Bell, E. B., and Miyan, J. A. (2004) Nerve fibres are required to evoke a contact sensitivity response in mice. *Immunology* **111,** 118–125
16. Banvolgyi, A., Palinkas, L., Berki, T., Clark, N., Grant, A. D., Helyes, Z., Pozsgai, G., Szolcsanyi, J., Brain, S. D., and Pinter, E. (2005) Evidence for a novel protective role of the vanilloid TRPV1 receptor in a cutaneous contact allergic dermatitis model. *J. Neuroimmunol.* **169,** 86–96
17. Yun, J. W., Seo, J. A., Jang, W. H., Koh, H. J., Bae, I. H., Park, Y. H., and Lim, K. M. (2011) Antipruritic effects of TRPV1 antagonist in murine atopic dermatitis and itching models. *J. Invest. Dermatol.* **131,** 1576–1579
18. Yun, J. W., Seo, J. A., Jeong, Y. S., Bae, I. H., Jang, W. H., Lee, J., Kim, S. Y., Shin, S. S., Woo, B. Y., Lee, K. W., Lim, K. M., and Park, Y. H. (2011) TRPV1 antagonist can suppress the atopic dermatitis-like symptoms by accelerating skin barrier recovery. *J. Dermatol. Sci.* **62,** 8–15
19. Shiba, T., Tamai, T., Sahara, Y., Kurohane, K., Watanabe, T., and Imai, Y. (2012) Transient receptor potential ankyrin 1 activation enhances hapten sensitization in a T-helper type 2-driven fluorescein isothiocyanate-induced contact hypersensitivity mouse model. *Toxicol. Appl. Pharmacol.* **264,** 370–376
20. Willis, D. N., Liu, B., Ha, M. A., Jordt, S. E., and Morris, J. B. (2011) Menthol attenuates respiratory irritation responses to multiple cigarette smoke irritants. *FASEB J.* **25,** 4434–4444
21. Man, M. Q., Hatano, Y., Lee, S. H., Man, M., Chang, S., Feingold, K. R., Leung, D. Y., Holleran, W., Uchida, Y., and Elias, P. M. (2008) Characterization of a hapten-induced, murine model with multiple features of atopic dermatitis: structural, immunologic, and biochemical changes following single versus multiple oxazolone challenges. *J. Invest. Dermatol.* **128,** 79–86
22. Johnson, K. R., Lane, P. W., Cook, S. A., Harris, B. S., Ward-Bailey, P. F., Bronson, R. T., Lyons, B. L., Shultz, L. D., and Davisson, M. T. (2003) Curly bare (cub), a new mouse mutation on chromosome 11 causing skin and hair abnormalities, and a modifier gene (mcub) on chromosome 5. *Genomics* **81,** 6–14
23. Wang, B., Fujisawa, H., Zhuang, L., Freed, I., Howell, B. G., Shahid, S., Shivji, G. M., Mak, T. W., and Sauder, D. N. (2000) CD4+ Th1 and CD8+ type 1 cytotoxic T cells both play a crucial role in the full development of contact hypersensitivity. *J. Immunol.* **165,** 6783–6790
24. Tsukumo, Y., Harada, D., and Manabe, H. (2010) Pharmacological characterization of itch-associated response induced by repeated application of oxazolone in mice. *J. Pharmacol. Sci.* **113,** 255–262
25. Kinkelin, I., Motzing, S., Koltenzenburg, M., and Brocker, E. B. (2000) Increase in NGF content and nerve fiber sprouting in human allergic contact eczema. *Cell Tissue Res.* **302,** 31–37
26. LaMotte, R. H., Shimada, S. G., and Sikand, P. (2011) Mouse models of acute, chemical itch and pain in humans. *Exp. Dermatol.* **20,** 778–782
27. Kuraishi, Y., Nagasawa, T., Hayashi, K., and Satoh, M. (1995) Scratching behavior induced by pruritogenic but not algesiogenic agents in mice. *Eur. J. Pharmacol.* 275, 229–233
28. Niwa, Y., Sumi, H., Kawahira, K., Terashima, T., Nakamura, T., and Akamatsu, H. (2003) Protein oxidative damage in the stratum corneum: Evidence for a link between environmental oxidants and the changing prevalence and nature of atopic dermatitis in Japan. *Br. J. Dermatol.* **149,** 248–254
29. Trevisani, M., Siemens, J., Materazzi, S., Bautista, D. M., Nassini, R., Campi, B., Imamachi, N., Andre, E., Patacchini, R., Cottrell, G. S., Gatti, R., Basbaum, A. I., Bunnett, N. W., Julius, D., and Geppetti, P. (2007) 4-Hydroxynonenal, an endogenous aldehyde, causes pain and neurogenic inflammation through activation of the irritant receptor TRPA1. *Proc. Natl. Acad. Sci. U. S. A.* **104,** 13519–13524
30. Neisius, U., Olsson, R., Rukwied, R., Lischetzki, G., and Schmelz, M. (2002) Prostaglandin E_2 induces vasodilation and pruritus, but no protein extravasation in atopic dermatitis and controls. *J. Am. Acad. Dermatol.* **47,** 28–32
31. Nojima, H., and Carstens, E. (2003) 5-Hydroxytryptamine (5-HT)2 receptor involvement in acute 5-HT-evoked scratching but not in allergic pruritus induced by dinitrofluorobenzene in rats. *J. Pharmacol. Exp. Ther.* **306,** 245–252
32. McQueen, D. S., Noble, M. A., and Bond, S. M. (2007) Endothelin-1 activates ETA receptors to cause reflex scratching in BALB/c mice. *Br. J. Pharmacol.* **151,** 278–284
33. Andoh, T., Katsube, N., Maruyama, M., and Kuraishi, Y. (2001) Involvement of leukotriene B(4) in substance P-induced itch-associated response in mice. *J. Invest. Dermatol.* **117,** 1621–1626
34. Rukwied, R., and Heyer, G. (1999) Administration of acetylcholine and vasoactive intestinal polypeptide to atopic eczema patients. *Exp. Dermatol.* **8,** 39–45
35. Andoh, T., Nishikawa, Y., Yamaguchi-Miyamoto, T., Nojima, H., Narumiya, S., and Kuraishi, Y. (2007) Thromboxane A2 induces itch-associated responses through TP receptors in the skin in mice. *J. Invest. Dermatol.* **127,** 2042–2047

36. Liang, J., Ji, Q., and Ji, W. (2011) Role of transient receptor potential ankyrin subfamily member 1 in pruritus induced by endothelin-1. *Neurosci. Lett.* **492,** 175–178
37. Carlton, S. M., Zhou, S., and Coggeshall, R. E. (1996) Localization and activation of substance P receptors in unmyelinated axons of rat glabrous skin. *Brain Res.* **734,** 103–108
38. von Banchet, G. S., and Schaible, H. G. (1999) Localization of the neurokinin 1 receptor on a subset of substance P-positive and isolectin B4-negative dorsal root ganglion neurons of the rat. *Neurosci. Lett.* **274,** 175–178
39. Li, H. S., and Zhao, Z. Q. (1998) Small sensory neurons in the rat dorsal root ganglia express functional NK-1 tachykinin receptor. *Eur. J. Neurosci.* **10,** 1292–1299
40. Tang, H. B., Li, Y. S., Arihiro, K., and Nakata, Y. (2007) Activation of the neurokinin-1 receptor by substance P triggers the release of substance P from cultured adult rat dorsal root ganglion neurons. *Mol. Pain* **3,** 42
41. Tang, H. B., Li, Y. S., Miyano, K., and Nakata, Y. (2008) Phosphorylation of TRPV1 by neurokinin-1 receptor agonist exaggerates the capsaicin-mediated substance P release from cultured rat dorsal root ganglion neurons. *Neuropharmacology* **55,** 1405–1411
42. Dunn, I. S., Liberato, D. J., Dennick, R. G., Castagnoli, N., and Byers, V. S. (1982) A murine model system for contact sensitization to poison oak or ivy urushiol components. *Cell. Immunol.* **68,** 377–388
43. Wakabayashi, T., Hu, D. L., Tagawa, Y., Sekikawa, K., Iwakura, Y., Hanada, K., and Nakane, A. (2005) IFN-γ and TNF-α are involved in urushiol-induced contact hypersensitivity in mice. *Immunol. Cell Biol.* **83,** 18–24
44. Honda, T., Egawa, G., Grabbe, S., and Kabashima, K. (2013) Update of immune events in the murine contact hypersensitivity model: toward the understanding of allergic contact dermatitis. *J. Invest. Dermatol.* **133,** 303–315
45. Grabbe, S., Steinert, M., Mahnke, K., Schwartz, A., Luger, T. A., and Schwarz, T. (1996) Dissection of antigenic and irritative effects of epicutaneously applied haptens in mice. Evidence that not the antigenic component but nonspecific proinflammatory effects of haptens determine the concentration-dependent elicitation of allergic contact dermatitis. *J. Clin. Invest.* **98,** 1158–1164
46. Caceres, A. I., Brackmann, M., Elia, M. D., Bessac, B. F., del Camino, D., D'Amours, M., Witek, J. S., Fanger, C. M., Chong, J. A., Hayward, N. J., Homer, R. J., Cohn, L., Huang, X., Moran, M. M., and Jordt, S. E. (2009) A sensory neuronal ion channel essential for airway inflammation and hyperreactivity in asthma. *Proc. Natl. Acad. Sci. U. S. A.* **106,** 9099–9104
47. Hosoi, J., Murphy, G. F., Egan, C. L., Lerner, E. A., Grabbe, S., Asahina, A., and Granstein, R. D. (1993) Regulation of Langerhans cell function by nerves containing calcitonin gene-related peptide. *Nature* **363,** 159–163
48. Andoh, T., Nagasawa, T., Satoh, M., and Kuraishi, Y. (1998) Substance P induction of itch-associated response mediated by cutaneous NK1 tachykinin receptors in mice. *J. Pharmacol. Exp. Ther.* **286,** 1140–1145
49. Togashi, Y., Umeuchi, H., Okano, K., Ando, N., Yoshizawa, Y., Honda, T., Kawamura, K., Endoh, T., Utsumi, J., Kamei, J., Tanaka, T., and Nagase, H. (2002) Antipruritic activity of the kappa-opioid receptor agonist, TRK-820. *Eur. J. Pharmacol.* **435,** 259–264
50. Scholzen, T. E., Steinhoff, M., Bonaccorsi, P., Klein, R., Amadesi, S., Geppetti, P., Lu, B., Gerard, N. P., Olerud, J. E., Luger, T. A., Bunnett, N. W., Grady, E. F., Armstrong, C. A., and Ansel, J. C. (2001) Neutral endopeptidase terminates substance P-induced inflammation in allergic contact dermatitis. *J. Immunol.* **166,** 1285–1291
51. El-Nour, H., Lundeberg, L., Al-Tawil, R., Granlund, A., Lonne-Rahm, S. B., and Nordlind, K. (2006) Upregulation of the axonal growth and the expression of substance P and its NK1 receptor in human allergic contact dermatitis. *Immunopharmacol. Immunotoxicol.* **28,** 621–631
52. Sundelin, J. B., Provvedini, D. M., Wahlestedt, C. R., Laurell, H., Pohl, J. S., and Peterson, P. A. (1992) Molecular cloning of the murine substance K and substance P receptor genes. *Eur. J. Biochem.* **203,** 625–631
53. Hesketh, P. J. (2008) Chemotherapy-induced nausea and vomiting. *N. Engl. J. Med.* **358,** 2482–2494
54. Duval, A., and Dubertret, L. (2009) Aprepitant as an antipruritic agent? *N. Engl. J. Med.* **361,** 1415–1416
55. Stander, S., Siepmann, D., Herrgott, I., Sunderkotter, C., and Luger, T. A. (2010) Targeting the neurokinin receptor 1 with aprepitant: a novel antipruritic strategy. *PloS One* **5,** e10968
56. Vincenzi, B., Tonini, G., and Santini, D. (2010) Aprepitant for erlotinib-induced pruritus. *N. Engl. J. Med.* **363,** 397–398
57. Mir, O., Blanchet, B., and Goldwasser, F. (2011) More on aprepitant for erlotinib-induced pruritus. *N. Engl. J. Med.* **364,** 487
58. Raap, U., Stander, S., and Metz, M. (2011) Pathophysiology of itch and new treatments. *Curr. Opin. Allergy Clin. Immunol.* **11,** 420–427
59. Atoyan, R., Shander, D., and Botchkareva, N. V. (2009) Non-neuronal expression of transient receptor potential type A1 (TRPA1) in human skin. *J Invest. Dermatol.* **129,** 2312–2315
60. Story, G. M., Peier, A. M., Reeve, A. J., Eid, S. R., Mosbacher, J., Hricik, T. R., Earley, T. J., Hergarden, A. C., Andersson, D. A., Hwang, S. W., McIntyre, P., Jegla, T., Bevan, S., and Patapoutian, A. (2003) ANKTM1, a TRP-like channel expressed in nociceptive neurons, is activated by cold temperatures. *Cell* **112,** 819–829
61. Hox, V., Vanoirbeek, J. A., Aguiar Alpizar, Y., Voedisch, S., Callebaut, I., Bobic, S., Sharify, A., De Vooght, V., Van Gerven, L., Devos, F., Liston, A., Voets, T., Vennekens, R., Bullens, D. M., De Vries, A., Hoet, P., Braun, A., Ceuppens, J. L., Talavera, K., Nemery, B., and Hellings, P. W. (2013) Crucial role of TRPA1 and mast cells in induction of non-allergic airway hyperreactivity in mice. *Am. J. Respir. Crit. Care Med.* **187,** 486–493
62. Fjellner, B., and Hagermark, O. (1981) Studies on pruritogenic and histamine-releasing effects of some putative peptide neurotransmitters. *Acta Derm. Venereol.* **61,** 245–250
63. Ekblom, A., Lundeberg, T., and Wahlgren, C. F. (1993) Influence of calcitonin gene-related peptide on histamine- and substance P-induced itch, flare and weal in humans. *Skin Pharmacol.* **6,** 215–222
64. Trentin, P. G., Fernandes, M. B., D'Orleans-Juste, P., and Rae, G. A. (2006) Endothelin-1 causes pruritus in mice. *Exp. Biol. Med. (Maywood)* **231,** 1146–1151
65. Imamachi, N., Park, G. H., Lee, H., Anderson, D. J., Simon, M. I., Basbaum, A. I., and Han, S. K. (2009) TRPV1-expressing primary afferents generate behavioral responses to pruritogens via multiple mechanisms. *Proc. Natl. Acad. Sci. U. S. A.* **106,** 11330–11335
66. Slominski, A., Wortsman, J., and Tobin, D. J. (2005) The cutaneous serotoninergic/melatoninergic system: securing a place under the sun. *FASEB J.* **19,** 176–194
67. El-Nour, H., Lundeberg, L., Abdel-Magid, N., Lonne-Rahm, S. B., Azmitia, E. C., and Nordlind, K. (2007) Serotonergic mechanisms in human allergic contact dermatitis. *Acta Derm. Venereol.* **87,** 390–396
68. Palm, N. W., Rosenstein, R. K., and Medzhitov, R. (2012) Allergic host defences. *Nature* **484,** 465–472

Received for publication February 27, 2013.
Accepted for publication May 14, 2013.

Suppl figure 1

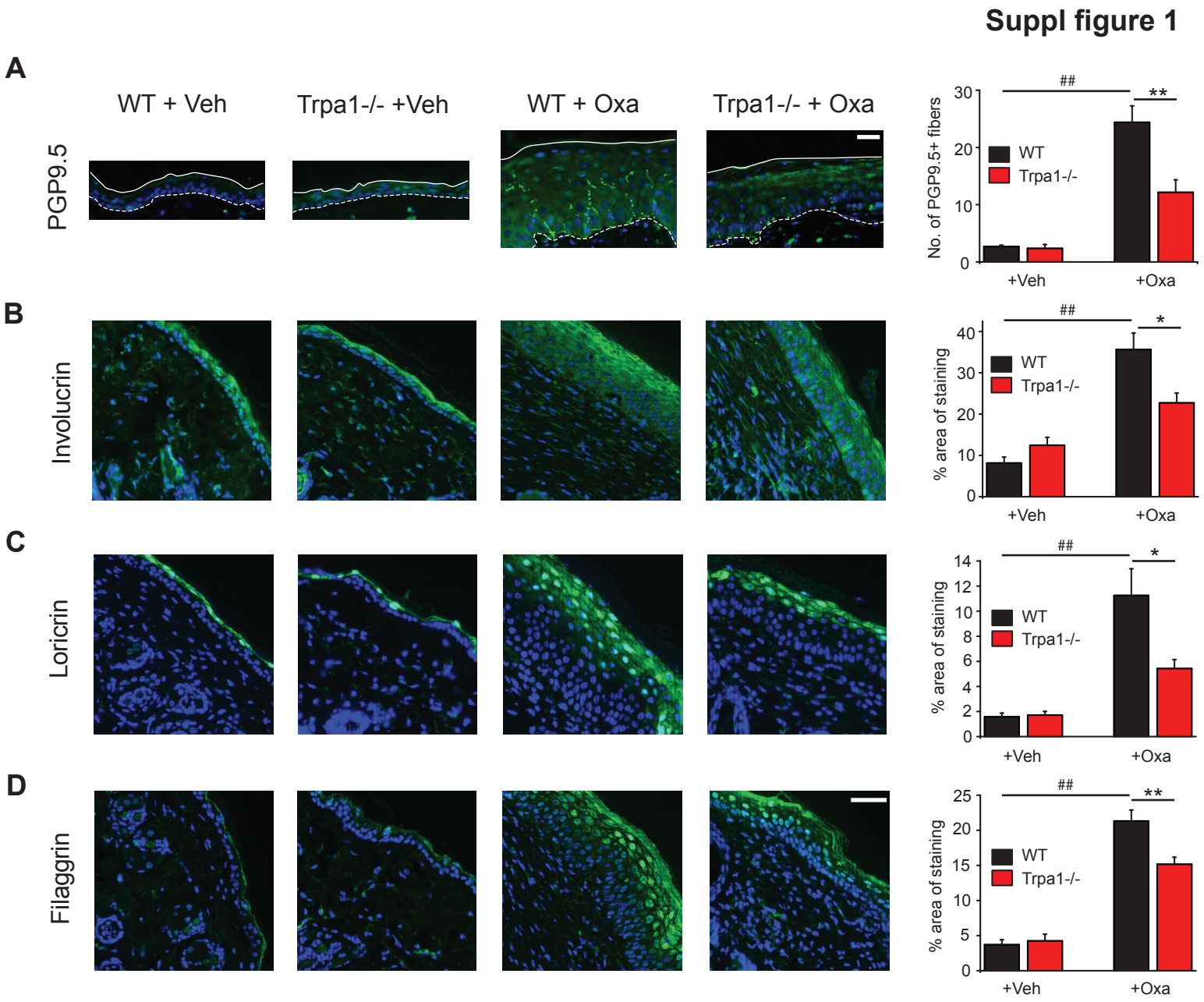

Suppl Fig. 1 Expression of structural markers of epidermal differentiation and cutaneous nerve fiber densities in wild-type and Trpa1-/- mice in oxazolone-induced dermatitis

(**A-D**) Representative immunofluorescence images of PGP9.5 positive (PGP9.5^{+}) nerve fibers (A involucrin (B), loricrin (C) and filaggrin (D) staining in the neck skin sections of WT and Trpa1-/- mice chronically challenged with acetone (Veh) or 0.5% oxazolone (Oxa) on the neck skin. Areas staining positive for involucrin, loricrin,filaggrin and PGP9.5 are shown in green. Nuclei were labeled with DAPI (purple). Data are summarized as % area of involucrin, loricrin and filaggrin staining and numbers of PGP9.5 positive nerve fibers. White and broken lines indicate the skin surface and the border between the epidermis and dermis, respectively. $^{\#\#}p < 0.01$, $^{**}p < 0.01$, $^{*}p < 0.05$. For (A), scale bar shows 50 µm. For (B-D), scale bar shows 20 µm. n = 6 to 12 mice/group.

Suppl figure 2

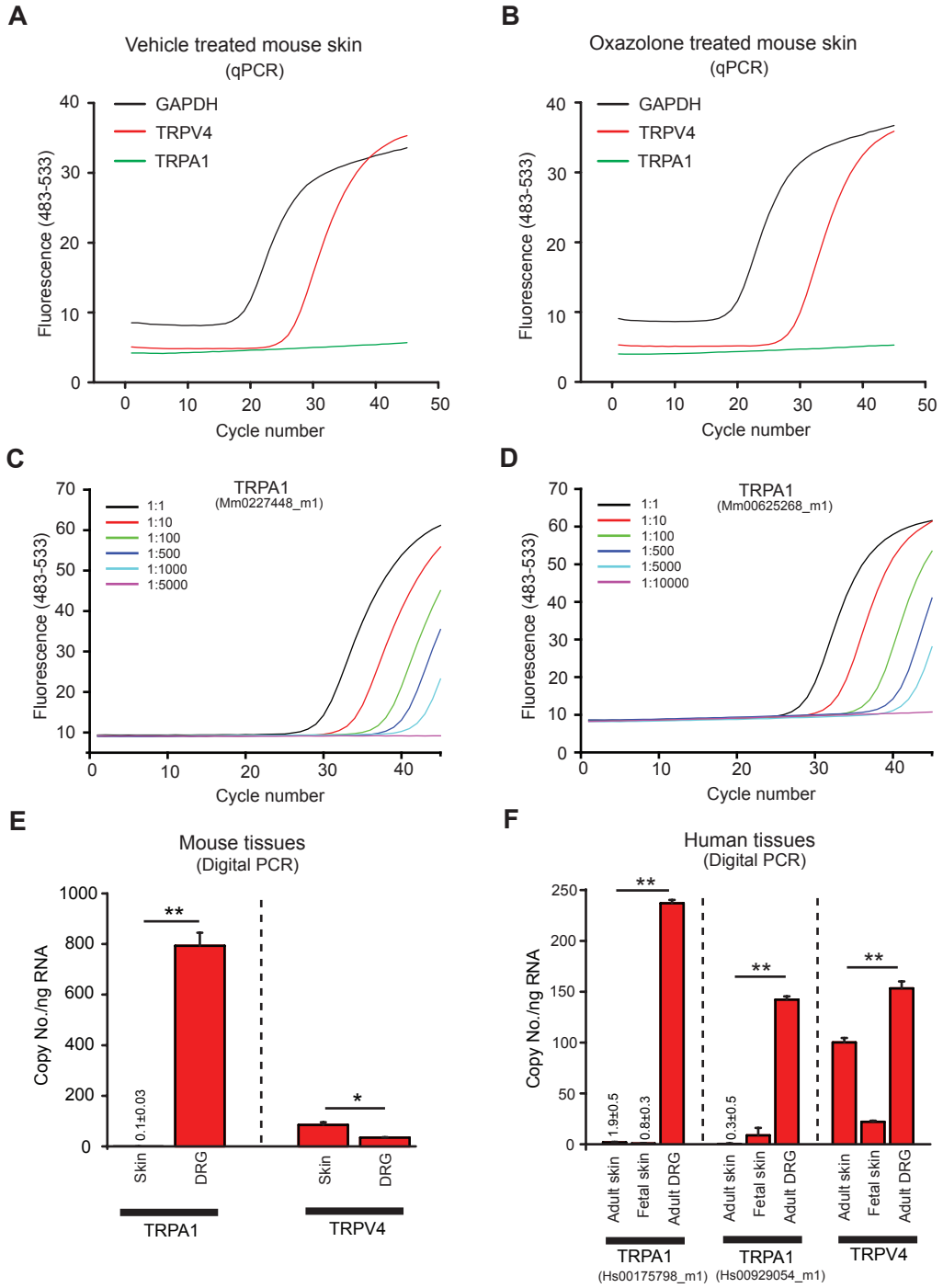

Suppl Fig.2 Analysis of TRPA1 channel gene transcription in mouse and human skin by quantitative real time PCR (qPCR) and digital droplet PCR (ddPCR)

(**A, B**) Representative qPCR fluorescence intensity traces comparing hydrolysis of probes for detection of GAPDH (black), TRPV4 (red) and TRPA1 (green) cDNAs in total cDNA generated from a neck skin biopsy of a mouse treated with vehicle (A) or chronically with oxazolone (B), plotted against cycle number. (**C, D**)Detection of TRPA1 cDNA in serial dilutions of DRG cDNA in skin cDNA.qPCR fluorescence intensity traces are shown comparing hydrolysis of Trpa1 probes Mm01227448_m1 (C) or Mm00625268_m1 (D). DRG cDNA was diluted 1:1–1: 10000 in skin cDNA. 1µg of combined cDNAs were used as template for each reaction. The hydrolysis probes detected TRPA1 cDNA at dilutions of 1:1000 and 1:5000, respectively. Since TRPA1 cDNA was not detected by the same probes in pure skin cDNA, this experiment demonstrates that DRGs contain 1000-5000-fold more TRPA1 message than skin. (**E**) Determination of TRPA1 cDNA copy numbers by ddPCR from mouse skin and DRG. n = 5 mice/group. Copy numbers were normalized to the amount of RNA (ng) used for reverse transcription. (**F**) Determination of TRPA1 cDNA copy numbers by ddPCR from adult/fetal skin and DRG of human. Two independent human TRPA1 probes are used as indicated. n = 5 tests/group. **$p < 0.01$, *$p < 0.05$.

Supplementary Figure 3

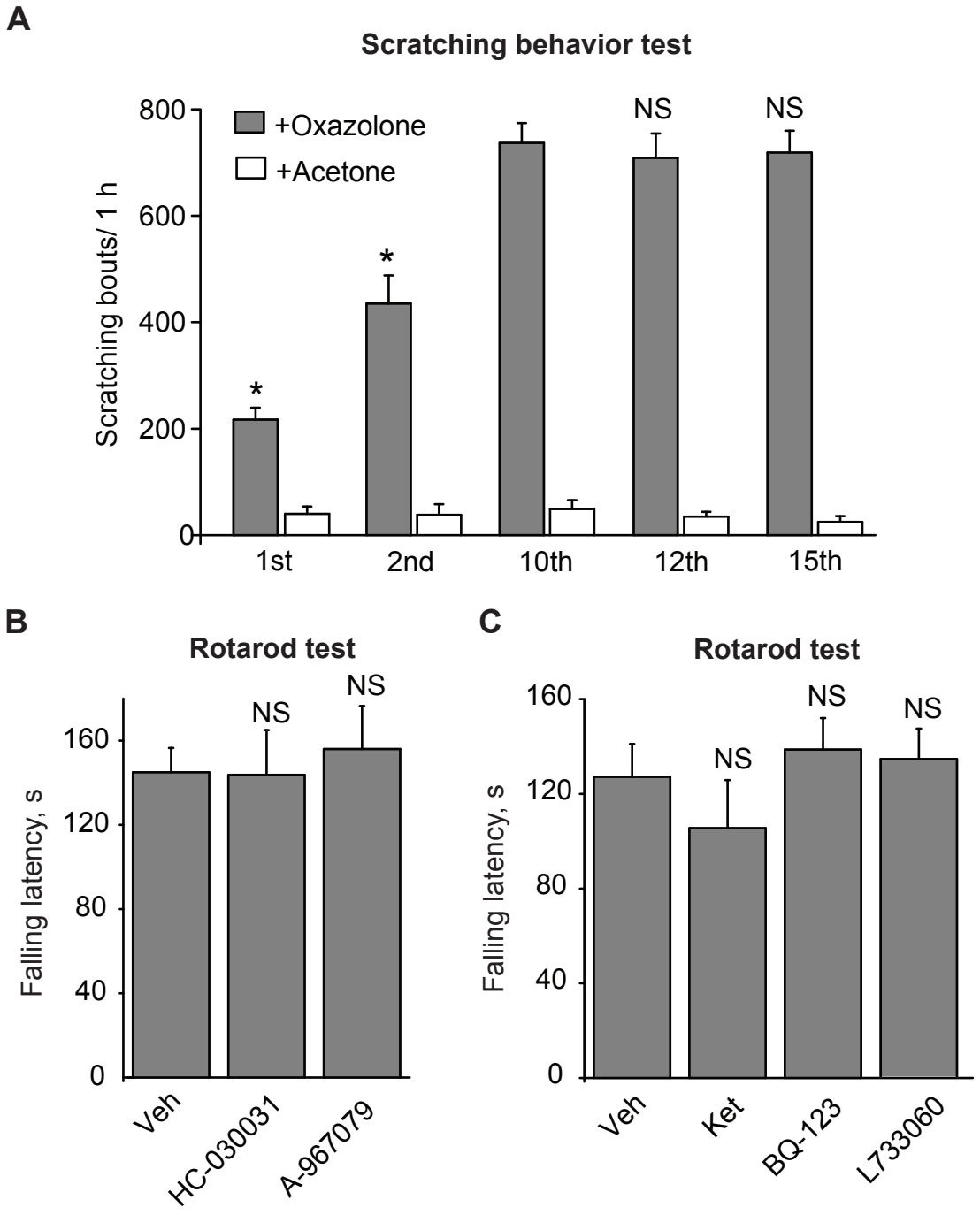

Suppl Fig.3 Scratching behavior following oxazolone application during establishment of chronic atopic dermatitis on the neck and effects of antipruritics and TRPA1 antagonists on mouse locomotor function tested by the accelerating rotarod test

(A) Quantities of scratching bouts following challenge of the neck skin with 0.5% oxazolone or acetone (vehicle), counted within 1 hour after the 1st, 2nd, 10th, 12th and 15th challenge during establishment of chronic atopic dermatitis. Mice were initially sensitized by application of 2% oxazolone. n = 5 mice/group. **$p < 0.05$ *vs*. the 10th challenge. **(B)** HC-030031 (60 mg/kg) and A-967079 (100 mg/kg) or vehicle was injected (i.p.) into mice 45 min before rotarod test. Mice were placed on a rotating cylinder with the speed increasing from 5 to 40 rpm within 5 min (IITC Inc.). Before drug testing mice were trained every day for 4 consecutive days. Mice showing only brief falling latencies during this period were excluded. During the test, each mouse was tested 3 times with an interval of 5 min between each test and the latency to fall was measured with a stopwatch. The falling latency listed is the averaged value of the 3 tests. n = 5 mice/group. **(C)** BQ123 (1 mg/kg), ketanserin (Ket, 3 mg/kg), L733060 (20 mg/kg) or vehicle was injected (i.p.) into mice 45 min before rotarod test. n = 5 mice/group. NS: not significantly different from vehicle group.

Suppl figure 4

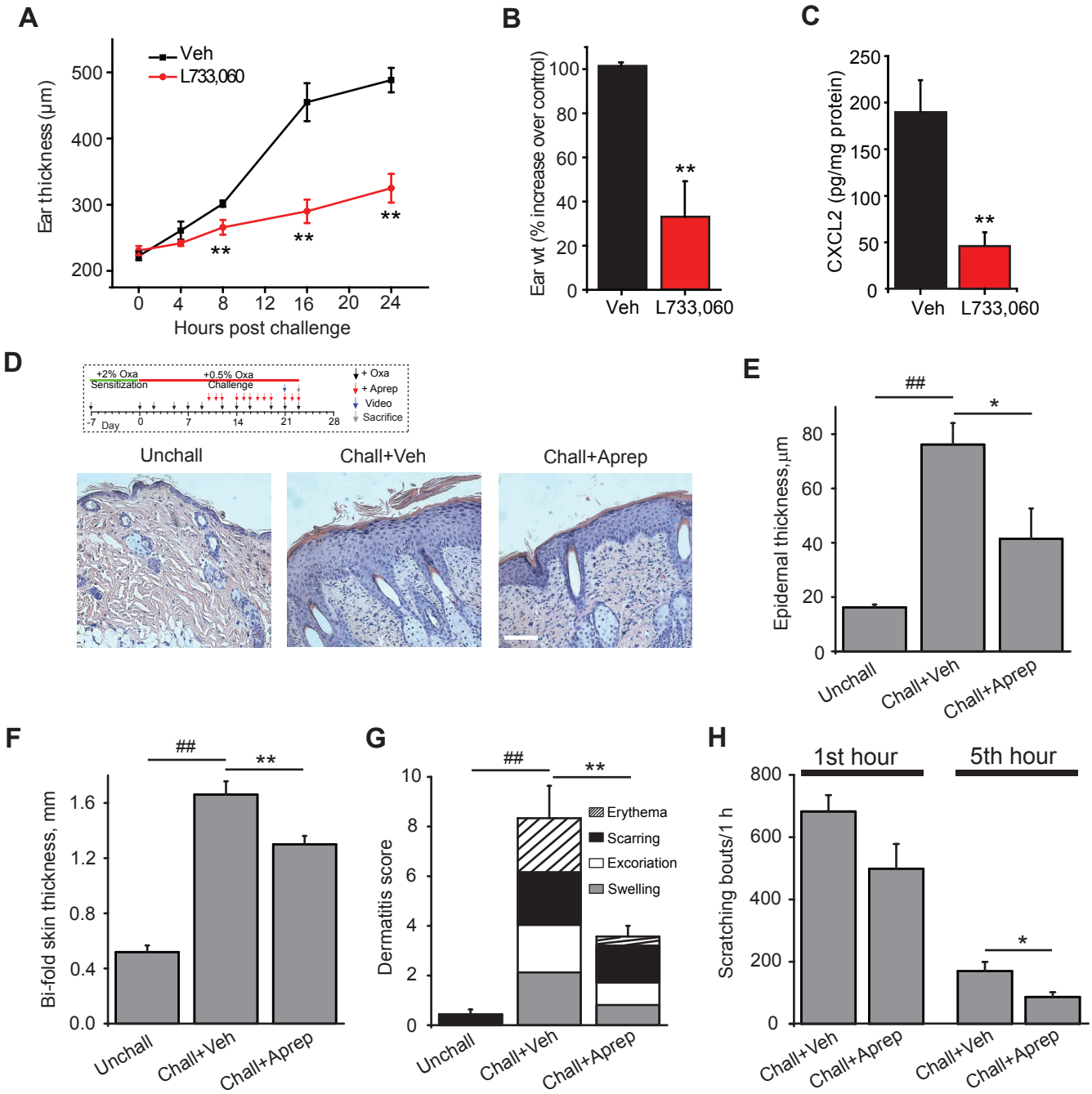

Suppl. Fig. 4 NK_1 receptor antagonists inhibits edema, inflammation and pruritus in acute and chronic oxazolone induced-dermatitis

(**A**) 24 h time course of ear thickness measurements in acute oxazolone-sensitized and ear-challenged mice treated with vehicle (Veh, 3% DMSO in PBS, i.p., black), or the NK_1 receptor antagonist, L733060 (red, 7.5 mg/kg, i.p.). n = 9 mice/group. (**B**) Comparison of weight increases of 4 mm ear punch biopsies from acute oxazolone challenged mice treated with vehicle (black) or L733060 (red), excised 24 h after challenge. Percent increases compared to biopsies of the unchallenged ears are shown. n = 9 mice/group. (**C**) Concentrations of the pro-inflammatory cytokine CXCL-2, in protein-extracts of ear punch biopsies, excised 24 h after acute oxazolone challenge from mice treated with vehicle (Veh, black), or L733060 (red), measured by ELISA. The cytokine was undetectable in samples from un-challenged mice. n = 9 mice/group. (**D**) H&E-stained sections of neck skin from unchallenged mice and chronic oxazolone challenged mice treated with vehicle (Veh) or aprepitant (Aprep, 10 mg/kg, i.p.). n = 7 to 8 mice/group. The inset shows the scheme of sensitization/challenge of mice with oxazolone and time points for treatments and measurements. (**E**) Measurements of epidermal thickness of unchallenged mice and chronic oxazolone challenged mice treated with vehicle or aprepitant. n = 7 to 8 mice/group. Scale bar represents 50 µm. (**F**) Comparison of bi-fold neck skin thickness of unchallenged mice (Unchall) and chronic oxazolone-challenged mice (Chall) treated with vehicle or aprepitant. n = 7 to 8 mice/group. (**G**) Averaged pathological dermatitis scores of unchallenged mice and chronic oxazolone-challenged mice treated with vehicle and aprepitant. n = 7 to 8 mice/group. (**H**) Numbers of scratching bouts within the 1st hour and 5th hour after the 10th application of oxazolone to mouse neck. Mice were treated with either vehicle or aprepitant 45 min before recording. n = 7 to 8 mice/group. $^{##}p < 0.01$, $^{*}p < 0.05$, $^{**}p < 0.01$.